# The effect of transcription factors on TAD boundaries in AML and upon myeloid differentiation – The HOXA locus

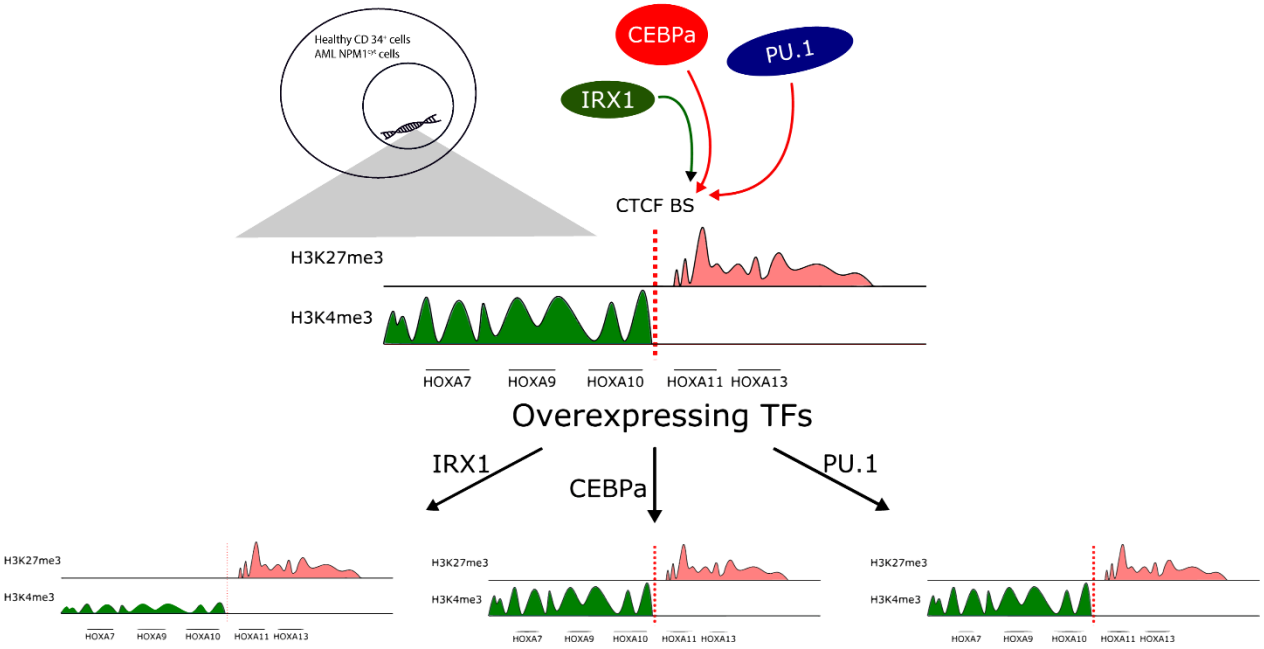



Author: W.S. van Midden
Supervisor: J.J. Schuringa
Daily supervisor: S.M. Hogeling
Date: 02-10-2019

*Department of Experimental Hematology*
*UMC Groningen*

## Abstract

Acute Myeloid Leukemia (AML) is a heterogeneous malignancy, characterized by impaired differentiation towards the myeloid lineage and an increased self-renewal ability. One of the most frequently mutated genes in AML is *NPM1* ($NPM1^{cyt}$), which is associated with aberrant *HOXA* expression, and in particular increased *HOXA9* expression.

ChIP-seq on primary AML patients samples in combination with hiC data showed the presence of a topologically associated domain (TAD) between the *HOXA10* and *HOXA11* genes on the *HOXA* locus. The majority of AML patients associated with an intact TAD boundary carried the $NPM1^{mut}$. This TAD boundary was also present in healthy $CD34^{+}$ cells, and was lost upon myeloid differentiation. Expression of *HOXA9* was typically associated with an intact TAD boundary as seen in normal $CD34^{+}$ cells and in leukemic blasts of $NPM1^{cyt}$ AML patients. $NPM1^{wt}$ AML patients have often lost the TAD boundary, as well as *HOXA9* expression. Analyzing the TCGA dataset showed that myeloid transcription factors (TFs) IRX1, CEBPa, and PU.1 possibly had a potential effect to remove TAD boundaries. Therefore, our hypothesis is that reintroduction or overexpression of TF activity in cells that have an intact TAD boundary will result in loss of the TAD boundary, repression of *HOXA* gene expression, and myeloid commitment. TAD boundaries are associated with CTCF binding sites and the cohesin complex, which consists out of four core-units: RAD21, STAG2, SMC1A, and SMC3. Therefore, we hypothesized that accelerated differentiation of $CD34^{+}$ can be initiated by knockdown of the cohesin genes or the *CTCF* gene to an impaired function of the TAD boundary.

Overexpression of CEBPa and PU.1 did not result in altered genetic expression on the *HOXA* locus, and did not alter the histone marks present on these loci. Furthermore, it did not induce differentiation of OCI AML3 cells. IRX1 overexpression in HEK 293T cells showed a decrease in *HOXA9* expression levels, downregulated H3K4me3 levels, and a decreased CTCF and RAD21 binding at the CTCF binding site. These results suggests that the TAD boundary was (at least partly) removed by IRX1 overexpression. Unfortunately, IRX1 overexpression in $CD34^{+}$ cells did not result in altered differentiation towards any lineage. KD of *CTCF* did not result in altered RAD21 binding at the TAD boundary, but resulted in highly upregulated HOXA genes in HEK 293T cells.

Altogether, these results shows that IRX1 could be a potential candidate to alter TAD boundaries in hematopoietic malignancies and upon differentiation.

# Contents

## Introduction

*The hematopoietic system*

Hematopoiesis is the process in which the cellular blood components are formed (Boisset & Robin, 2012). At the apex of the hematopoietic hierarchy, the hematopoietic stem cell (HSC) is found, which resides in the bone marrow and is multipotent. HSCs are mostly quiescent, and have the ability to self-renew (Bradford et al., 1997; Morrison et al., 1997). HSCs numbers are relatively small, since the estimated frequencies of HSCs in the bone marrow is 1:10.000 cells and in the peripheral blood it is 1:100.000 blood cells (Ng et al., 2009). However, a single HSC had the ability to reconstitute the entire hematopoietic system in irradiated mice, which is why HSCs are used for bone marrow transplantations in hematological malignancies (Birbrair & Frenette, 2017; Matsuzaki et al., 2004; Osawa et al., 1996). It was proposed that HSCs were the only cells responsible for blood cell production, however, another study found that in normal native conditions, the production of blood was mainly maintained by multipotent progenitors in micec (MPPs) (J. Sun et al., 2014; Weissman, 2000). However, the hematopoietic compartment always experiences at least minimal stress levels, so it might be that in humans HSCs are still mainly responsible for blood production. A new study proposed that there are different regulatory mechanisms that regulates and maintain the different output of high regenerative potential blood cells in humans (Knapp et al., 2018).

HSCs can be divided into three different populations, the long-term hematopoietic stem cell (LT-HSC), the intermediate-term HSC (IT-HSC), and the short-term HSC (ST-HSC) (Figure 1). They differ in their self-renewal capacity and activity (Benveniste et al., 2010; Yamamoto et al., 2013). ST-HSCs differentiate towards multipotent progenitors, which consist of different subpopulations (MPP2, MPP3, and MPP4/LMPP) (Zhang, Gao, Xia, & Liu, 2018). It was thought that MPPs were responsible for the division between the myeloid and lymphoid lineages, but recent studies have shown that the fate of LT-HSCs is probably already predetermined at the embryonic stage (Kester & van Oudenaarden, 2018; Macaulay et al., 2016; Tang et al., 2017). The MPP2 and MPP3 cells mainly generate common myeloid progenitors (CMPs), whereas MPP4s differentiate towards common lymphoid progenitors (CLPs). The CMP can give rise to matured hematopoietic cells via the megakaryocyte/erythrocyte progenitor (MEP) or the granulocyte/macrophage progenitor (GMP). CLPs are responsible for mature lymphoid cells, however mature lymphoid cells can also derive from MPP4s directly (Pietras et al., 2015).

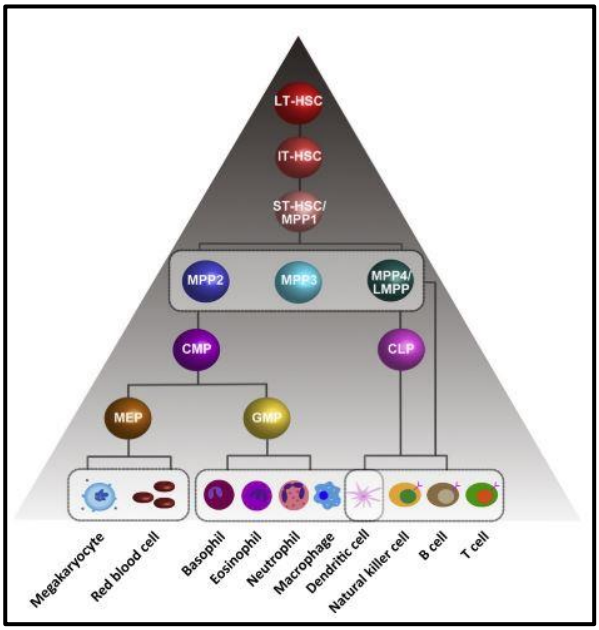

Figure 1. The hematopoietic hierarchy (Zhang et al., 2018)

*Acute myeloid leukemia*

In acute myeloid leukemia (AML) patients, the differentiation towards the myeloid lineage is blocked, while the self-renewal ability is increased. AML is a very heterogeneous malignancy, driven by different genetic and epigenetic mutations. Interestingly, the average number of mutations in AML patients was only 13, which is actually fewer than most other human cancers (Cancer Genome Atlas Research

Network, 2013). AML patients often had more than one somatically acquired driver mutation (86%), which promote cancer development (Papaemmanuil et al., 2016). Mutations that encode for epigenetic modifiers, like *DNMT3A*, *TET2*, and *IDH1/2* were often acquired in early disease progression (Corces-Zimmerman et al., 2014; Papaemmanuil et al., 2016). These early mutations targeted hematopoietic transcription factors, leading to impaired myeloid differentiation and an aberrant self-renewal ability (Alharbi et al, 2013). Mutations in proliferative genes occurred late and caused disease progression. They affected signaling pathways like *FLT3* and enhanced proliferation signal transduction pathways, resulting in an increased HSC proliferation (Alharbi et al., 2013; Corces-Zimmerman et al., 2014; Papaemmanuil et al., 2016).

*HOX* genes are one of those frequently overexpressed transcription factors, and especially the *HOXA9* gene is upregulated in almost half of the AML patients (Collins & Hess, 2016; Collins et al., 2014; Golub et al., 1999). Upregulation of *HOXA* and *B* genes was highly associated with *NPM1* mutations ($NPM1^{cyt}$), which is next to *FLT3* and *DNMT3A* one of the most frequently mutated genes in AML (Alcalay et al., 2005; Cancer Genome Atlas Research Network, 2013). Another subset of mutated genes in AML consist of mutations of the cohesin complex genes (*RAD21*, *SMC1A*, *SMC3*, and *STAG2*), and were first reported in 2012 (Ding et al., 2012). These mutations were mutually exclusive, and were found in 6-12% of AML samples (Cancer Genome Atlas Research Network, 2013; Kon et al., 2013; Thol et al., 2014).

### *HOX genes in normal hematopoiesis and leukemia*

*HOX* genes are mainly known for their regulatory role during embryogenesis in animals, since they encoded for transcription factors that are essential for the embryonic process (Gentile & Kmita, 2018; Krumlauf, 1994). By this, *HOX* genes make sure that the correct structures are developed on the correct spot of the body. There are 39 *HOX* genes in mammals, which are organized into four different clusters (A-D), all located on four different chromosomes: 7p15 (*HOXA*), 17q21 (*HOXB*), 12q13 (*HOXC*), and 2q31 (*HOXD*) (Rice & Licht, 2007).

Next to their role in early development, *HOX* genes also play a role in hematopoiesis. The *HOX* genes were mainly expressed in hematopoietic stem cells and their immature progenitors, and were downregulated during hematopoietic differentiation (Lawrence & Largman, 1992; Moretti et al., 1994). These genes were furthermore lineage- and differentiation dependent, whereby *HOXA* genes were expressed in myeloid cells, *HOXB* genes in erythroid cells and *HOXC* in lymphoid cells (Alharbi et al., 2013). *HOXD* genes were not expressed during hematopoiesis. Important *HOX* genes for HSC-maintenance were *HOXB4* and *HOXA9*, since overexpression of both of these genes resulted in increased self-renewal and HSC expansion (Buske et al., 2002; Thorsteinsdottir et al., 2002). Interestingly, *HOXB4* did not result in (hematological) malignancies or shifted cell commitment, whereas *HOXA9* overexpression led to AML and a differential preference towards the myeloid lineage. Furthermore, *HOXA9* depletion led to impaired hematopoiesis in the form of reduced cell commitment towards the myeloid and erythroid lineage (Lawrence et al., 1997). Of all *HOX* genes, *HOXA9* was the most expressed *HOX* gene in human $CD34^{+}$ cells (Alharbi et al., 2013). As mentioned before, *HOXA9* expression was upregulated in a significant subset of human AMLs and when mutated, associated with a poor prognosis (Alharbi et al., 2013; Golub et al., 1999).

During normal hematopoiesis, the *HOXA9* expression is regulated by the transcriptional activator MLL (mixed-lineage leukemia), which is responsible for methylation of H3K4 along the *HOXA9* gene (M. W. M. Kühn et al., 2016; R. C. Rao & Dou, 2015). MLL recruits menin and its cofactor LEDGF in order to deposit H3K4me3. Dysregulation or mutation of MLL can result in hematological malignancies, thereby recruiting DOT1L, which is an H3K79 methyl transferase (Milne et al., 2005; Okada et al., 2005). This may drive dysregulated *HOXA9* expression and results in AML (Krivtsov & Armstrong, 2007). Next to MLL-fusion proteins, aberrant *HOXA9* expression was also regulated by upstream alterations NUP98-fusions,

MOZ-CBP-fusions, *CDX2* overexpression, and NPM1$^{cyt}$ (Camós et al., 2006; Falini et al., 2009; Nakamura et al., 1996).

### *Topologically associated domains*

Chromatin organization is another regulator of the *HOXA* genes (Gentile & Kmita, 2018). The genome is divided into topologically associated domains (TADs), regulating the interaction between different parts of the genome (Cremer & Cremer, 2001). There are two different TADs, an active (A) and an inactive (B) compartment (Lieberman-aiden et al., 2009). The active compartment is characterized by higher chromatin accessibility and transcriptional activity, whereas the inactive compartment has a lower transcriptional activity due to the more densely packed chromatin form (and thereby less accessible) and the presence of H3K27me3 (Rao et al., 2014). Furthermore, active TADs are found more inside the cell's nucleus, whereas the repressed domains mainly resides near the nuclear lamina (Guelen et al., 2008; Matharu & Ahituv, 2015). Within these TADs are regions that have enriched chromatin interactions, named subTADs (Phillips-Cremins et al., 2013; S. S. P. Rao et al., 2014). This could explain why genes within the same TAD had different expression levels and states (active or inactive) (Cubeñas-Potts & Corces, 2015).

At the border of each TAD, there is a so called TAD boundary. These TAD boundaries have a barrier function, preventing spreading of heterochromatin or epigenetic modifications to connected TADs, and thereby preventing interaction between genes (Dixon et al., 2012). TAD boundaries are modulated by and enriched for the insulator protein CCCTC-binding factor (CTCF) and the cohesin complex (Dixon et al., 2012; Nora et al., 2012; Pope et al., 2014). CTCF binding sites are required for cohesin to bind at the DNA (Mirny et al., 2016; Wendt et al., 2008). This cohesin complex consists of the four subunits: RAD21, SMC3, SMC1A, and STAG2 (Hill, Kim, & Waldman, 2016).

In healthy cord blood CD34$^{+}$ cells, TAD boundaries were present on the *HOXA* locus between *HOXA10* and *HOXA11*, and were lost upon myeloid differentiation (van den Boom et al., 2016; Yi et al., 2019). However, in the majority of AML patients with NPM1$^{cyt}$, this TAD boundary was still present which consequently results in dysregulated expression of *HOXA9* and *HOXA10*.

Another study showed that a TAD boundary was located between *HOXA7* and *HOXA9* in 3 subtypes of AML patients (including NPM1$^{cyt}$ and MLL-rearranged leukemia), similarly to the position of TAD boundaries in mouse- and human ESCs (Dixon et al., 2012; Luo et al., 2018). These TAD boundary-associated AML subtypes can be divided in NPM1$^{cyt}$/*FLT3-ITD*$^{+}$, MLL rearrangements and gain-of-copy MLL mutations. In the study of Luo *et al.* (2018), they removed the CTCF binding site via CRISPR/CAS on the TAD boundary present between the *HOXA7* and *HOXA9* gene, which was sufficient to remove the TAD boundary completely. After removal of the TAD boundary, H3K27me3 was transferred towards the posterior active TAD. By transferring H3K27me3 towards the active TAD, which contained the *HOXA9* gene, *HOXA9* is repressed, and therefore differentiation was initiated again.

### *The role of transcription factors on HOXA expression*

The myeloid transcription factor PU.1 is an essential regulator for monocytes and contributes to granulocytic differentiation (Henkel et al., 1999; Iwasaki et al., 2005). PU.1 collaborates with CEBPa and RUNX1, two other myeloid transcription factors, to drive granulomonocytic differentiation (Hohaus et al., 1995; Hu et al., 2011). In NPM1$^{cyt}$ AML cells, PU.1 was dislocated with the mutated NPM1 from the cell's nucleus into the cytoplasm (Gu et al., 2018). CEBPa and RUNX1 remained nuclear, and their protein interactomes were enriched for the transcription repressors like DNMT1 and CBX. Interestingly, PU.1 negatively correlated with *HOXA9* expression during myelopoiesis. Reintroduction of PU.1 into the cell nucleus resulted in myeloid differentiation, and downregulated *HOXA9* expression. Next to PU.1 overexpression, CEBPa overexpression in AML cells (HF-6; Kasumi-1; SKH-1) upregulated myeloid differentiation genes and repressed stem cell function genes like *HOXA9* (Loke et al., 2018; Matsushita et

al., 2008). Furthermore it is shown that at the *HOXA9* binding sites, CEBPa motifs were enriched, suggesting a direct role of CEBPa in *HOXA9* regulation (C. Collins et al., 2014; Y. Sun et al., 2018). Another transcription factor that showed a potential role to alter *HOXA9* expression after analyzing the TCGA dataset, is IRX1 (Figure 2A) (Cancer Genome Atlas Research Network, 2013). Furthermore, Bloodspot analysis showed a decreased IRX1 expression in MLL-rearranged leukemias (like NPM1$^{cyt}$), which are associated with high HOXA9 levels and an intact TAD boundary, thereby suggesting a role for IRX1 in TAD boundary biology (Haferlach et al., 2010; Kohlmann et al., 2008; Rapin et al., 2014; Svendsen et al., 2016).

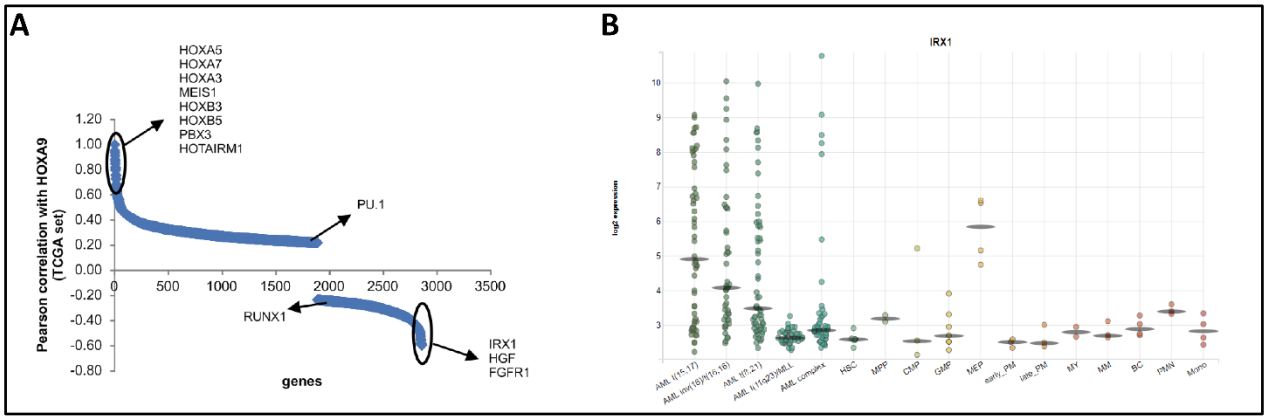


**Figure 2. (A)** Pearson correlation for *HOXA9* from the TCGA dataset. Interesting genes are highlighted in the picture, with a special interest in IRX1 and PU.1. **(B)** Expression levels of IRX1 in different AMLs and during normal hematopoiesis.

### *The aim of the study*

In this study we investigated whether the TAD boundary on the *HOXA* cluster can be depleted by overexpressing myeloid transcription factors (TFs) CEBPa, PU.1 and IRX1. Our hypothesis is that reintroduction or overexpression of TF activity in cells that have an intact TAD boundary will result in loss of the TAD, repression of *HOXA* gene expression, and myeloid commitment. Furthermore, we want to understand the role of the cohesin complex in this context, and we hypothesize that if we knockdown one of the cohesin genes or the *CTCF* gene, differentiation in normal CD34$^{+}$ cells is faster induced due to an impaired function of the TAD boundary.

Since *HOXA9* is often upregulated in NPM1$^{cyt}$ AML patients, we make use of the OCI AML3 and IMS M2 cell line, because they have a NPM1$^{cyt}$ and an intact TAD boundary as well. Furthermore, we will transduce CD34$^{+}$ cells derived from cord blood and follow these cells during differentiation. Our focus is primarily on *HOXA* expression, histone marks on the *HOXA* locus, and the effects on myeloid differentiation and the cohesin complex. The used workflow is shown in Figure 3A, whereas the used viral constructs are shown in Figure 3B.

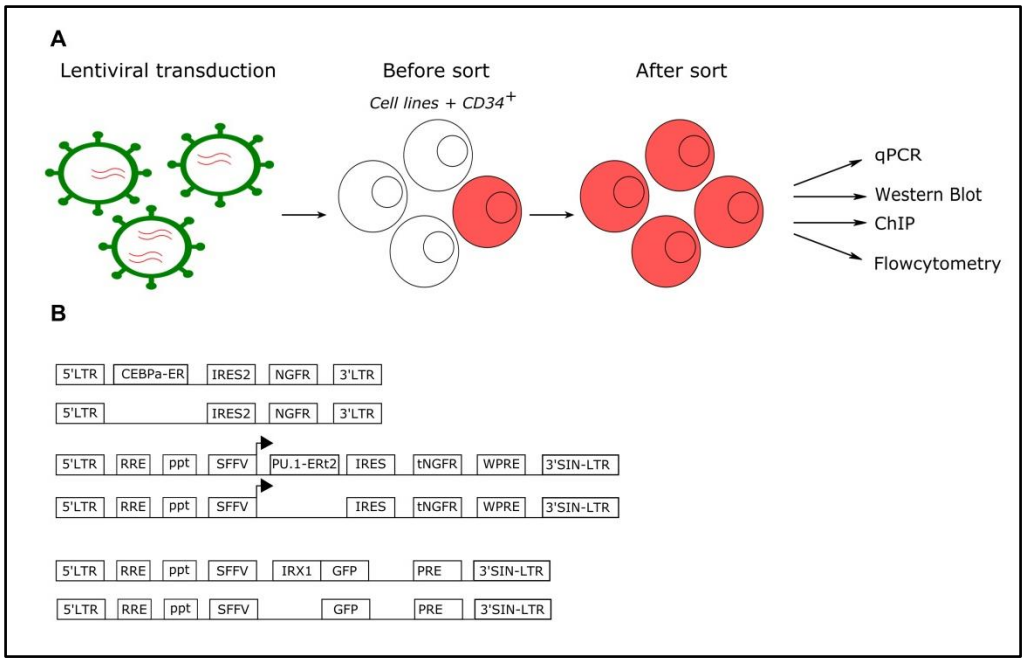


**Figure 3. (A)** Schematic representation of the workflow. Cells were transduced, sorted, and cultured. After different time points, samples were taken for RT-qPCR, Western Blot, ChIP, or flow cytometry. **(B)** Schematic representation of retroviral (CEBPa-ER) and lentiviral (PU.1-ER and IRX-GFP) constructs that were used in these studies. The CEBPa-ER construct was originating from Wierenga et al., 2010, the PU.1-ER construct originates from Korthuis et al., 2015, and the IRX-GFP from GenScript. CEBPa-ER and PU.1-ER inducible constructs and are activated with 4-Hydroxytamoxifen (4-OHT; Sigma-Aldrich) treatment, since heat shock proteins are then released from the ER, and the CEBPa-ER or PU.1-ER can enter the nucleus. The empty vectors MinR1-ER, NGFR-ER, and EV-GFP were control constructs for CEBPa-ER, PU.1-ER, and IRX-GFP respectively.

## Material and methods

**Cell culture**
Leukemic cell lines HL60, K562, and IMS M2 were cultured in RPMI 1640 (Lonza) with 10% Fetal Calf Serum (FCS) (Sigma-Aldrich) and 1% penicillin/strepromycin (P/S) (Gibco). OCI AML3 cells were cultured in αMEM (Lonza) with 20% FCS and 1% P/S. HEK 293T cells were cultured in DMEM (Gibco) with 10% FCS and 1% P/S. All cells were cultured at 37 °C with 5% $CO_2$.

**CD34$^+$ isolation from cord blood**
Cord blood was received from the Martini Hospital and the University Medical Centre in Groningen, the Netherlands. Blocking- (FcR) and CD34$^+$ beads (Miltenyi Biotech) were added before sorting on the autoMACS Pro Separator (Miltenyi Biotech). Cells were sorted into a CD34+ and CD34- fraction. Before transduction, CD34$^+$ cells were cultured for 1 day, with 1 ml Stemline (SAFC) with 1% P/S, supplemented with 20ng/mL TPO, 20ng/mL c-Kit (SCF), and 20 ng/mL FLT-3.

**CD34$^+$ differentiation**
Isolated and transduced CD34$^+$ cells were cultured in IMDM (Gibco) with 20% FCS, 1 % P/S and supplemented with 20 ng/mL stem cell factor (SCF). In order to get differentiation towards the myeloid lineage, 20 ng/mL IL-3 was added. For the granulocyte lineage, 20 ng/mL IL-3 and 20 ng/mL G-CSF were added. To differentiate towards the erythroid lineage, 3 U/mL EPO was added. Cells were analyzed for cell surface markers CD11b, CD14, CD15, CD114, CD71, and CD235a, viability, and GFP percentage via flow cytometry on day 0, 4, 6, 8, and 12.

**Lenti- and retroviral transduction**
For lentiviral transduction, 293T cells were transfected with PAX, VSV-G, Fugene (Promega) and the PU.1-ER, NGFR-ER, IRX1-GFP, EV-GFP, shCTCF-III or the shSCR construct (Figure 3B, 9A). Virus was harvested after 48 hours and passed over a 40 µM filter to remove residual HEK 293T cells. Transduction in the OCI AML3, IMS M2, HL60, K562 cell lines was performed by adding viral supernatant in a ratio of 1:4 with αMEM or RPMI in a 6-well plate, with 8 µg/ml polybrene (Sigma-Aldrich). HEK 293T cells were transduced in a 1:4 ratio with 8 µg/ml polybrene. For CD34$^+$ transduction, 0.2 x $10^6$ CD34$^+$ cells in 0.5 ml Stemline II were supplemented with 0.5 ml viral supernatant, 2 - 4 µg/ml polybrene, and cytokines (as described previously), in a pre-coated 24-wells plate with retronectin, and spinoculated for 45 min at 800 RPM. After 24 hours, cells were collected.
Retroviral transduction was performed for CEBPa-ER and MinR1-ER after generating a stable PG13 retroviral producer cell line. Viral supernatant was collected from PG13 cells and passed over a filter, before cells were transduced in three consecutive rounds (+ 8 µg/ml polybrene). Transduction efficiency of cells transduced with CEBPa-ER or PU.1-ER was measured on the BD Accuri C6 Flow Cytometer (BD Biosciences) using the CD271-PE antibody. Transduction efficiency of IRX1-GFP/EV-GFP or shCTCF/shSCR transduced cells were measured on the BD Accuri C6 Flow Cytometer or the BD LSR-II (BD Biosciences) for GFP or mCherry fluorescence, respectively. If the transduction efficiency was less than 95%, cells were sorted.

**shRNA generation**
To generate shRNA for *CTCF* and cohesin genes, we cloned 3 sequences per gene into the pLKO.1 backbone in combination with a mCherry tag. Generated shRNAs were transduced into HEK 293T cells to test their knockdown efficiency. A scrambled shRNA (shSCR) was used as control. The used shRNA sequence for CTCF-III was 5'-TTGGGAAGGACTTAGAGTTTTATAAAACTCTAAGTCCTTCCCAA-3'.

**RNA isolation, cDNA synthesis and quantitative Reverse-Transcription Polymerase Chain Reaction**
For total RNA isolation, the QIAGEN RNeasy® Plus Mini or Micro Kit protocol was used. After RNA isolation, RNA concentration was measured by Nanodrop 1000 (Thermo Fisher Scientific). 200-2000 µg RNA was used for cDNA synthesis using the iScript™ cDNA Synthesis Kit (Bio-Rad). The cDNA reaction was incubated in a thermal cycler using the following protocol: priming for 5 min at 25°C, Reverse transcription (RT) for 20 min at 46°C, RT inactivation for 1 min at 95°C. To determine mRNA expression levels, qRT-PCR was performed on the CFX384 Touch Real-Time PCR Detection System (BioRad), using SsoAdvanced™ Universal SYBR® Green Supermix (Bio-Rad). One

cycle contained 1 minute on 95 °C (denaturation) and 1 min on 58 °C (annealing). This was 45 times repeated. Used primer sequences can be found in supplemental table 1. Each qRT-PCR was performed in triplicate. Relative expression changes were determined with the $2^{-\Delta\Delta CT}$ method, and normalized with the housekeeping gene RPL27.

**Western Blot analysis**

Ideally, 500.000 cells were used for Western Blot. For whole cell lysates, cell pellets were resuspended directly in 2X sample buffer. Buffer A was used to separate the nuclear and cytoplasmic fractions. Samples were loaded on Mini-PROTEAN® TGX™ Precast Gels (Bio-Rad) for electrophoresis. Protein transfer from the gel to a PVDF membrane was done by using the RTA Transfer Kit (Bio-Rad) in a Trans-Blot Turbo Transfer System (Bio-Rad) for 7 min at 25V (1.3A). The membrane was blocked for 30-60 minutes at room temperature with 5% Skim milk powder in Tris-buffered saline containing 0.1% Tween-20 (TBS-T) (Bio-Rad). After blocking, the membrane was incubated overnight with the primary antibody (1:500-1:2000) at 4 °C. The HPR-conjugated secondary antibody in blocking buffer was added (1:2000) and incubated for 1-2 hours. To develop the signal, SuperSignal West Pico PLUS Chemiluminescent Substrate (ThermoFisher) in a ratio of 1:1 was added onto the membrane, before visualizing the HRP activity on the ChemiDoc XRS+ (Bio-Rad) followed by analyzing using the Image Lab 6.0.1. (Bio-Rad). Used antibodies can be found in supplemental table 2.

**Cytospin**

50.000 cells were selected for cytospin, using the Shandon Cytospin 3 (Marshall Scientific). Samples were air-dried overnight before May-Grünwald Giemsa (MGG) staining. Representative pictures were taken on the Leica DM 3000.

**Flow cytometry**

To analyze cell differentiation, an amount of 20.000 – 200.000 cells was used. Antibodies for myeloid markers were added (supplemental table 2) and incubated for 20-30 minutes at 4 °C. Cells were measured on the MACSQuant® analyzer 10 (Miltenyi Biotech) or on the BD LSR-II (BD Biosciences). Data was analyzed using FlowJo 10 (FlowJo, LLC) and visualized using GraphPad Prism 8.2.0 (GraphPad Software).

**Chromatin Immunoprecipitation**

Chromatin Immunoprecipitation (ChIP) was essentially performed as described previously (Frank et al., 2001). In our study, ChIP was performed on OCI AML3-MinR1-ER, OCI AML3-CEBPa-ER, OCI AML3-NGFR-ER, OCI AML3-PU.1-ER, K562-NGFR-ER, K562-PU.1-ER, HEK 293T-EV-GFP and HEK 293T-IRX1-GFP cells. Cells were cross-linked with 1% formaldehyde. After shearing and purification of the DNA, antibodies specific for histone marks (α-H3K4me3, α-H3K27me3, α-H3K27ac) and proteins (α-CTCF, α-RAD21) were added. α-IgG was used as a control. Antibody- or protein-DNA complexes were isolated after which the cross-links were reversed. DNA was purified with the Qiagen PCR-clean-up kit and analyzed using qRT-PCR. Used antibodies and buffers are found in supplemental table 2 and 3. Exact locations of ChIP primers can be found in supplemental figure 3 and 4.

**Statistical analysis**

The paired t test was performed to calculate statistical differences. $P < 0.05$ was considered statistical significant. $P^* < 0.05$, $P^{**} < 0.01$, $P^{***} < 0.001$. Error bars show the standard deviation.

## Results

**50nM 4-OHT and 100nm 4-OHT was sufficient to induce CEBPa and PU.1 overexpression, respectively**

In order to determine whether the 4-OHT inducible transcription factors (CEBPa-ER and PU.1-ER) were properly transduced into the cell lines, we first measured the expression of the NGF receptor by flow cytometry. The transduced cells were >90% positive for the NGFR compared to non-transduced cells, except for IMS M2 PU.1-ER (35%) and K562 PU.1-ER (67%) transduced cells (Supplemental Figure 1). Furthermore, we confirmed proper transduction and overexpression by Western Blot by analyzing protein levels (Figure 4A).

By treating the cells with 4-Hydroxytamoxifen (4-OHT), heat shock proteins will be released from the ER, whereby the CEBPA-ER and PU.1-ER protein can enter the nucleus, resulting in overexpression of these transcription factors (Korthuis et al., 2015; Wierenga, Vellenga, & Schuringa, 2010). To determine which 4-OHT concentration resulted in overexpression of transcription factors, we treated the cells with different concentrations of 4-OHT, and measured the expression of different target genes (Figure 4B-4C). A concentration of 100 nM 4-OHT was sufficient to increase CSF3R, CT2 and CALCRL expression in the OCI AML3 PU.1-ER cell line. In HL60 PU.1-ER, CSF3R and CT2 were, surprisingly, downregulated. CSF3R was also upregulated in K562 PU.1-ER cells, however CT2 expression levels were not very affected, except for the 100 nM 4-OHT concentration. CSF3R is normally upregulated after PU.1 overexpression, therefore we did not take the HL60 PU.1-ER cell line into our panel (Korthuis et al., 2015). Since it was intended as a control cell line, it did not affect our study. What was interesting as well, was that CT2 would be thought to be downregulated as shown in HL60, however that was not the case in OCI AML3 (Korthuis et al., 2015). Based on this experiment and the previous study, we decided to continue with a concentration of 100 nM 4-OHT for the following experiments with PU.1-ER cells. To validate CEBPa activity, we analyzed the expression of CEBPa target genes *PU.1*, *RUNX1*, and *SIRPa*. In OCI AML3, IMS M2, and K562, PU.1 expression was already 2-45 times upregulated after addition of 50 nM 4-OHT. Once again, the HL-60 cells showed an aberrant pattern in gene expression compared to the other cell lines. Since 50 nM 4-OHT was sufficient to increase the expression of target genes, we decided to continue with this concentration for the upcoming experiments.

**CEBPa overexpression in OCI AML3 cells results in slightly more myeloid committed cells, but does not induce differentiation**

After we validated our cell lines and confirmed that CEBPa and PU.1 are overexpressed after addition of 4-OHT, we analyzed the effect of CEBPa on *HOXA* genes. We hypothesized that overexpression would result in lowered *HOXA9* expression, and that this would be due to increased H3K27me3 levels or decreased H3K4me3 levels on the *HOXA9* locus. We studied the *HOXA9* and *HOXA10* expression, and we took *MEIS1* into account since MEIS1 cooperates with HOXA9 (Lasa et al., 2004). There was no significant change in expression levels for *HOXA9* after 72 hours of stimulation with 4-OHT in OCI AML3 CEBPa-ER (Figure 5A). However, *HOXA10* expression was slightly upregulated, and *MEIS1* expression was 2.5-fold upregulated compared to the control. Since induction for 72 hours with 4-OHT was maybe not sufficient to induce changes in *HOXA* gene expression, we took mRNA samples after 5, 10, and 12 days. There was a minor change in *HOXA9* expression after 10 days, and *HOXA10* expression was first slightly upregulated before downregulated on day 12 (Figure 5B). *HOXA11* expression was upregulated on day 5, however the effect was lost on day 10 and day 12. Except for the *HOXA11* expression, these results matched mRNA samples which were taken on day 4, 6, and 11 (Supplemental Figure 2A). Despite the lack of significant changes in *HOXA* gene expression, we decided to perform chromatin immunoprecipitation (ChIP) to analyze the histone marks on several places on the *HOXA* locus at different time points (supplemental figure 3 and 4). The presence of the active histone mark H3K4me3 was not significantly affected on the

*HOXA9-11* genes, on both day 3 and day 5 (Figure 5C-D). Moreover, the active H3K4me3 mark seemed even to be slightly enhanced on the *HOXA9* locus. Regarding the repressive H3K27me3 mark, the signals were too low and the IgG levels too high for correct interpretation.

To analyze if CEBPa overexpression was able to induce (myeloid) differentiation, despite the lack of effect on (epi)genetic levels, we checked myeloid cell surface markers in OCI AML3. Surprisingly, the median fluorescence intensity (MFI) of CD11b, CD15, and CD13 was higher in CEBPa overexpressing cells than in the control (Figure 5E). However, after analyzing cytospin samples which were taken after 10 days, we did not see a clear distinction in differentiation status and cell morphology (Figure 5F).

Altogether, our data showed that CEBPa overexpression did not influence *HOXA9* expression, but it upregulated *HOXA10*, *HOXA11*, and *MEIS1* expression. Furthermore, it enhanced the H3K4me3 marks at the *HOXA10* locus, possibly explaining the upregulation of *HOXA10*. According to the upregulated *SIRPα* expression and higher MFI of myeloid cell surface markers, we could suggest that CEBPa overexpression initiated differentiation. However, cells morphology did not show any difference in differentiation status, implicating that overexpression of CEBPa initiated differentiation in OCI AML3, but that there is another mechanism that blocks the definite differentiation.

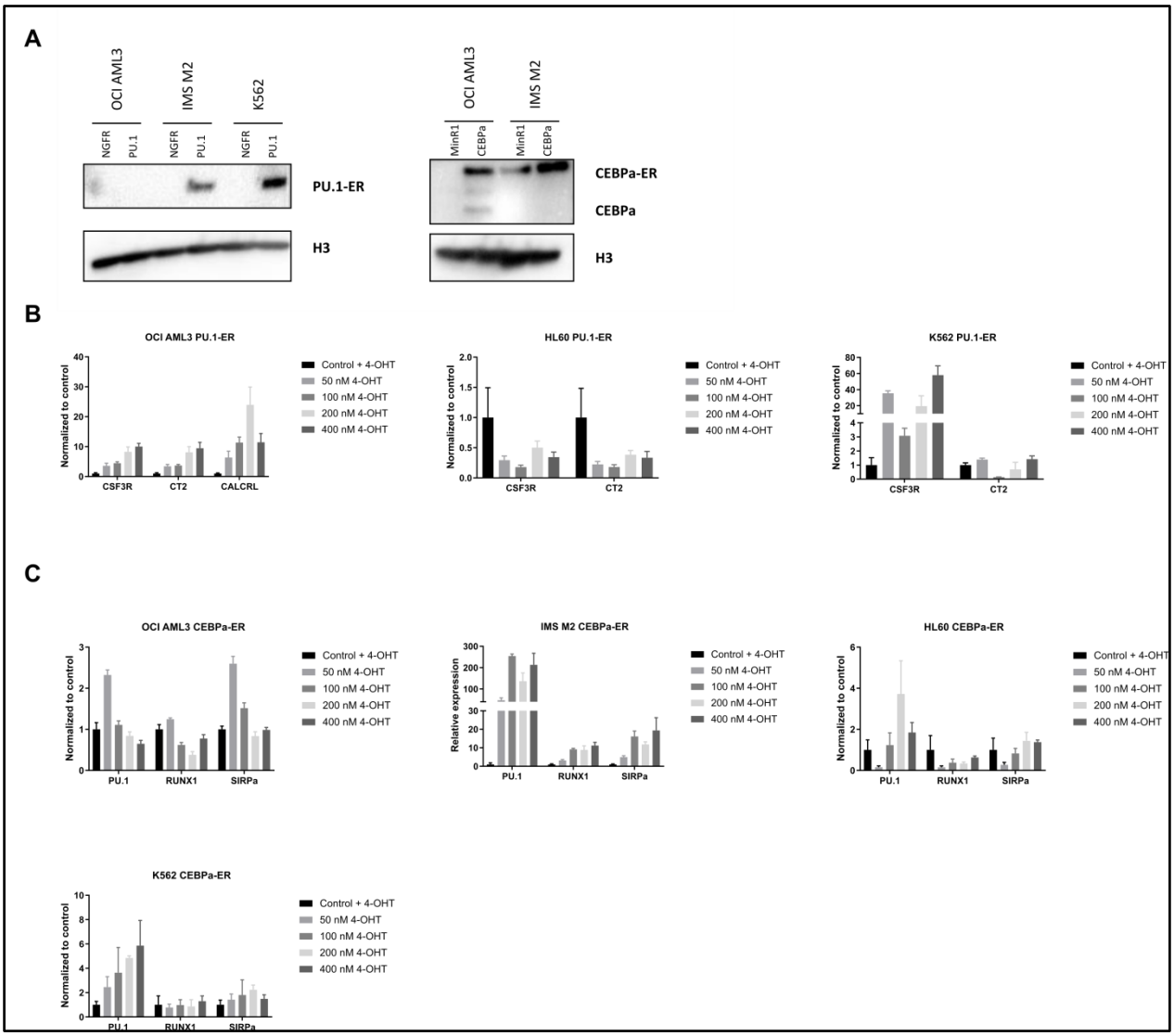

**Figure 4. 50nM 4-OHT and 100nm 4-OHT was sufficient to induce CEBPa-ER and PU.1-ER overexpression, respectively.** All data was derived with n = 1. **(A)** 500.000 cells were used for Western Blot. Whole-cell lysates were analyzed after 24h of 4-OHT induction for overexpression of CEBPa and PU.1. **(B)** qPCR results of OCI AML3, HL60, and K562 cells after PU.1-ER transduction. Relative expression levels of PU.1 target genes (*CSF3R*, *CT2*, *CALCRL*) were measured after 24h induction with different concentrations of tamoxifen (4-OHT) and normalized against the NGFR-ER transduced accessory cell line **(C)** qPCR results of OCI AML3, IMS M2, HL60, and K562 cells after CEBPa-ER transduction. Expression levels of CEBPa target genes (*PU.1*, *RUNX1*, *SIRPa*) were measured after 24h induction with different concentrations of 4-OHT and normalized against the MinR1-ER transduced accessory cell line.

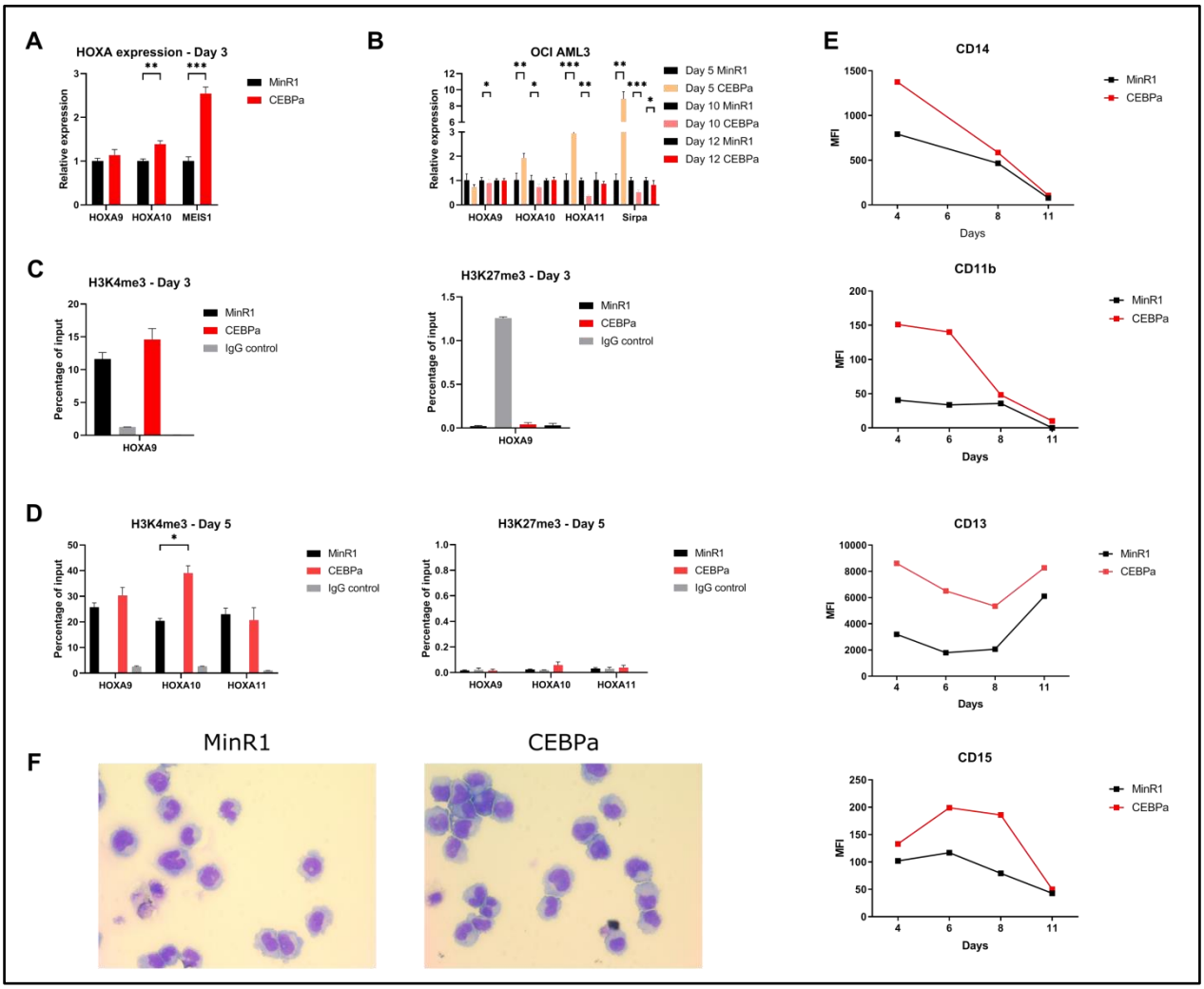


**Figure 5. CEBPa overexpression in OCI AML3 cells results in slightly more myeloid committed cells, but does not induce differentiation.** All experiments in this figure were done in OCI AML3 transduced with CEBPA-ER or MinR1-ER as control. All data was derived with n = 1. Exact ChIP locations can be found in supplemental figure 3. . **(A)** qPCR results of *HOXA* and *MEIS1* gene expression levels after 3 days of 4-OHT induction. **(B)** qPCR results of *HOX* genes and the CEBPa target gene *SIRPA*. mRNA was isolated after 5, 10 and 12 days with 4-OHT. **(C)** After 3 days with 4-OHT induction, 4 x $10^6$ cells were cross-linked for 10 minutes before ChIP was performed for histone marks H3K4me3 and H3K27me3. Obtained genomic DNA was used for the RT-qPCR for the *HOXA9* loci. IgG serves as control. **(D)** Same experiment as in C, but now cells were induced for 5 days with 4-OHT, and multiple loci were analyzed. **(E)** Median fluorescence intensity (MFI) of the myeloid and granulocytic markers CD14, CD11b, CD15, and CD13 were measured on day 4, 6, 8, and 11 of 4-OHT induction by FACS on the MACSQuant 10. **(F)** 50.000 cells were used for Cytospin after 10 days of 4-OHT induction. Representative pictures of samples were taken.

**Overexpression of PU.1 has a minimal effect on *HOXA* expression and does not induce myeloid differentiation**

Although it seemed that CEBPa overexpression resulted in slightly more myeloid committed OCI AML3 cells, it probably didn't affect the TAD boundary, and therefore we continued with another transcription factor, PU.1. After 3 days of treatment with 4-OHT, there was no notable change in *HOXA9* expression, and *HOXA10* and *MEIS1* were slightly downregulated compared to the control in OCI AML3 cells (Figure 6A). Longer induction with 4-OHT induced higher *HOXA9* expression after 10 and 12 days, combined with downregulation of *HOXA10* and *HOXA11* at the same the same days (Figure 6B, supplemental Figure 2B). The highest effect was notable on day 10, and on day 12 it was already less distinct. After treating K562 PU.1-ER cells with 4-OHT, *HOXA9* expression was remarkably upregulated (Figure 6C). However, under normal conditions, K562 cells did not have measurable amounts of *HOXA9* expression, or at least very low expression (Lawrence et al., 1999). Therefore, we presumed that the increased *HOXA9* expression was due to these low normal expression. Furthermore, PU.1 overexpression did not result in *HOXA9* expression changes in HEK 293T cells, but it increased *HOXA7* expression and led to downregulation of *HOXA10* and *MEIS1* (Figure 6D).

Although *HOXA9* expression was not changed in OCI AML3 cells after 3 days of 4-OHT treatment, we still performed a ChIP on these cells. Similarly to CEBPa overexpression, H3K4me3 levels were not significantly changed and H3K27me3 levels were not present (Figure 6E). H3K4me3 marks were only slightly decreased after 5 days of PU.1 overexpression on the *HOXA9* locus, but that was not seen after 10 days (Figure 6F). Furthermore, there were no clear changes of H3K4me3 marks on *HOXA10* or *HOXA11*. Despite the fact that K562 cells did not show *HOXA9* expression in normal conditions, we were still wondering if the upregulation of *HOXA9* was due to epigenetic changes. Since *HOXA9* expression was linked to TAD biology, we hypothesized that PU.1 overexpression resulted in an increased TAD boundary in these cells. However, overexpression of PU.1 did not altered epigenetic marks on the *HOXA5-11* locus (Figure 6G).

Next, we investigated if PU.1 overexpression resulted in differentiation of OCI AML3 cells by analyzing cell surface markers and the morphology of the cells. After 4 days, the MFI of myeloid- and granulocytic surface markers CD14, CD11b, and CD13 was higher compared to the control cells (Figure 6H). Though, the effect diminished over time. Furthermore, analyzing the cell morphology of PU.1 overexpressing cells did show a difference in differentiation after 10 days of 4-OHT induction. (Figure 6I).

These results indicate that PU.1 does not influence *HOXA9* expression by altering the TAD boundary in OCI AML3 cells.

**OCI AML3 cells do not have the same epigenetic landscape as found in AML patients, but HEK 293T cells do**

Since both CEBPa and PU.1 overexpression did not result in the expected (epi)genetics changes, we were wondering if OCI AML3 cells had the same epigenetic landscape as we previously found in AML patients. Interestingly, ChIP-seq data of OCI AML3 compared to AML patient data showed that the epigenetics of OCI AML3 cells were significantly different compared to AML patient data (Brunetti et al., 2018; van den Boom et al., 2016) (Figure 7A). The repressive H3K27me3 mark was not present throughout the whole *HOXA* locus, whereas H3K4me3 was found on *HOXA7-A13*, suggesting that our expected TAD boundary was not present. Next, we found that HEK 293T cells had a similar epigenetic landscape (ENCODE), and there was a TAD boundary between *HOXA10* and *HOXA11* as well (Figure 7B). Therefore, we decided to continue with HEK 293T cells instead of OCI AML3 cells to see if we can alter the TAD boundary by overexpressing TFs. Once we find an appropriate TF candidate, we will transduce this TF into CB $CD34^+$ cells. According to the dataset found in Figure 7B, H3K27ac was a good epigenetic marker as well in HEK 293T cells, so we will continue studying this histone marker in addition to H3K4me3 and H3K27me3.

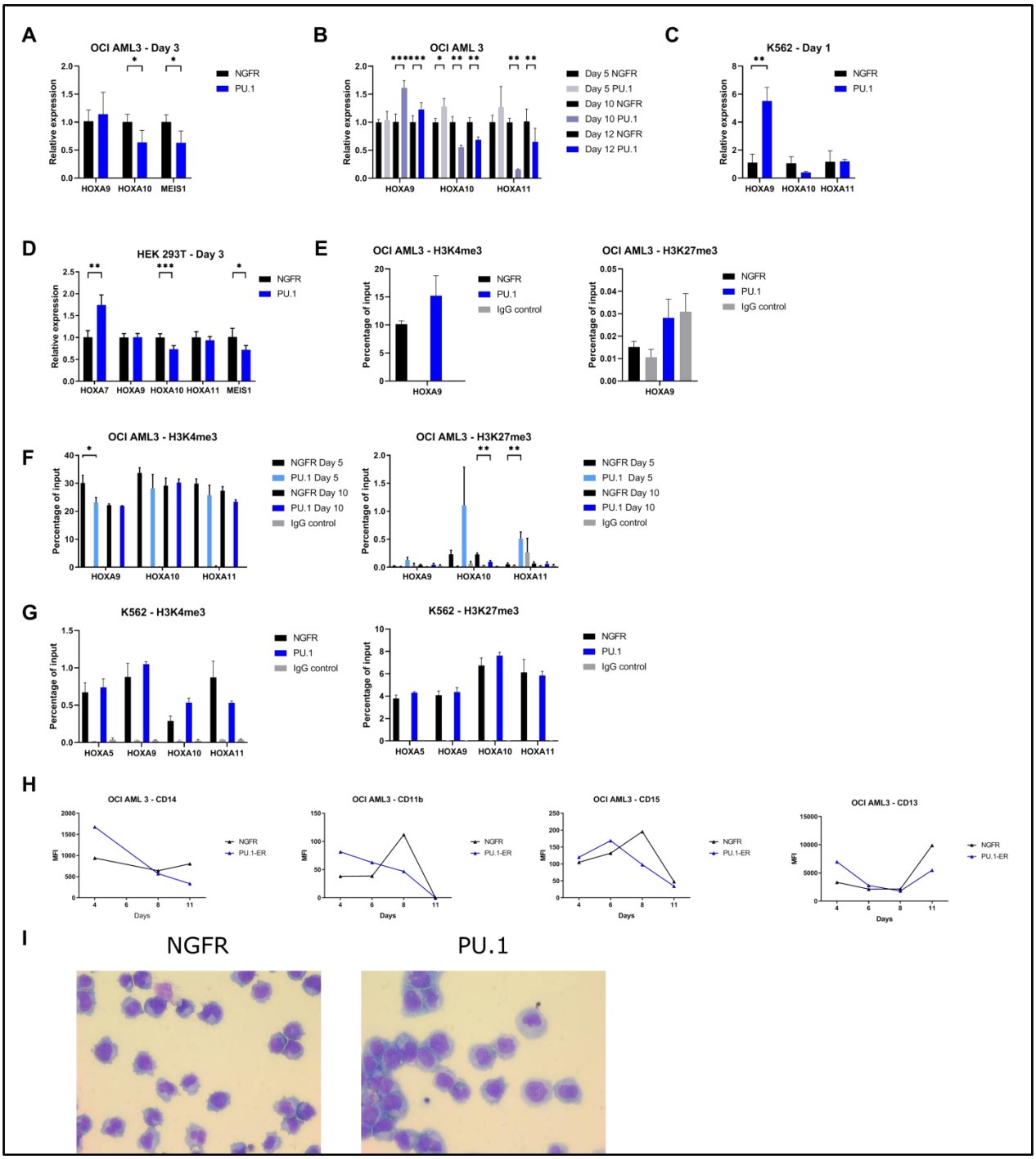


**Figure 6. Overexpression of PU.1 has a minimal effect on *HOXA* expression and does not induce myeloid differentiation.** All data was derived with n = 1, and exact ChIP locations can be found in supplemental figure 3. **(A)** qPCR of OCI AML3 cells after 3 days of 4-OHT treatment. **(B)** qPCR of OCI AML3 with 4-OHT, with samples taken on day 5, 10, and 12. **(C)** qPCR of K562 cells after 1 day of 4-OHT treatment. **(D)** qPCR of HEK 293T cells after 3 days of 4-OHT treatment. **(E)** qPCR of ChIP samples taken on day 3 with 4-OHT treatment for H3K4me3 and H3K27me3 in OCI AML3 cells. **(F)** ChIP qPCR after day 5 and 10 of 4-OHT treatment on OCI AML3 cells. **(G)** ChIP qPCR after day 7 days of 4-OHT treatment in K562 cells. **(H)** Median fluorescence intensity (MFI) of the myeloid and granulocytic markers CD14, CD11b, CD15, and CD13 were measured on day 4, 6, 8, and 11 of 4-OHT induction by FACS on the MACSQuant 10. **(I)** 50.000 cells were used for Cytospin after 10 days of 4-OHT induction. Representative pictures of samples were taken.

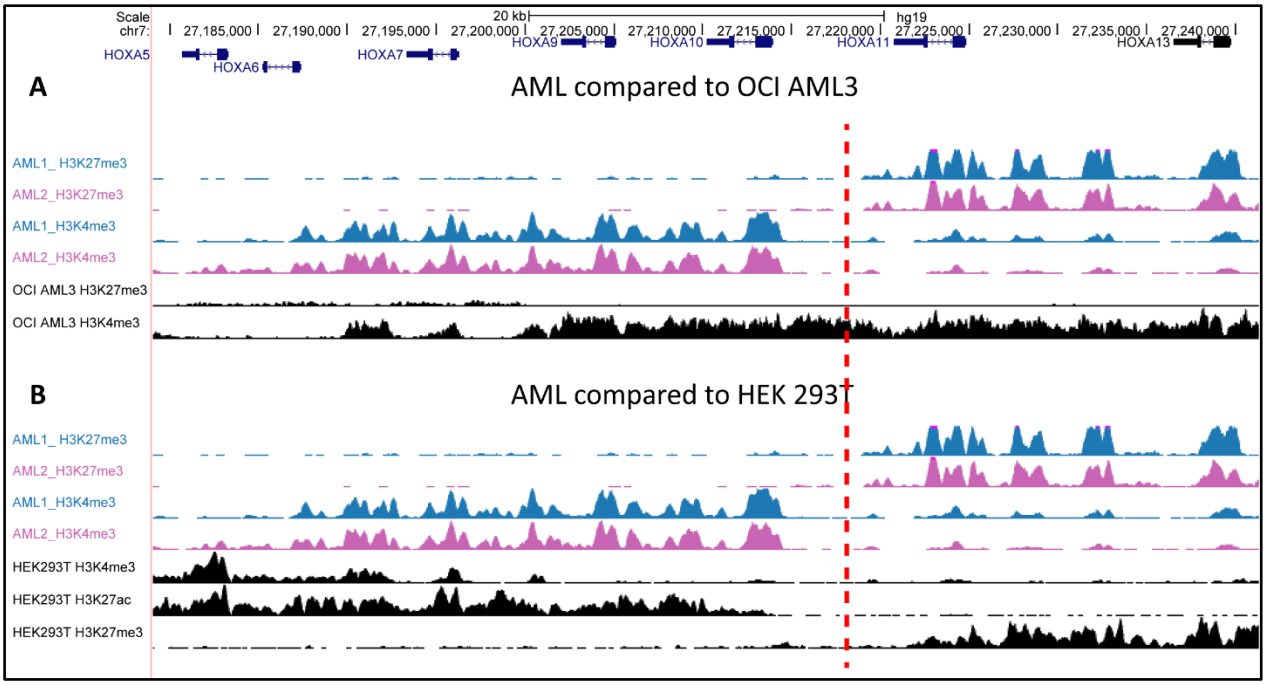


**Figure 7. OCI AML3 cells do not have the same epigenetic landscape as found in AML patients, but HEK 293T cells do** (Brunetti et al., 2018; van den Boom et al., 2016; ENCODE)**. (A)** ChIP-seq of AML patients for H3K27me3 and H3K4me3, compared to ChIP-seq data of OCI AML3. The red line indicates the TAD boundary. **(B)** ChIP-seq of AML patients for H3K27me3 and H3K4me3 compared to ChIP-seq data of HEK 293T cells. The ChIP-seq for H3K27ac indicates that H3K27ac is a good marker to analyze TAD boundary alterations in HEK 293T cells.

**IRX1 overexpression in HEK 293T cells downregulates *HOXA9* and an alters CTCF and RAD21 binding at CBS A10/11**

A study of Kühn *et al.* (2016) showed that IRX1 overexpression leads to a downregulation of HOXA9 expression in HEK 293T cells. This result, in combination with the ENCODE data, our data, and data from the TCGA set (Cancer Genome Atlas Research Network, 2013), could suggest that the IRX1 overexpression induced downregulation of *HOXA9* was caused by altered TAD boundaries. Therefore, we first confirmed that our IRX1 overexpression was present and overexpressed in cells using WB (Figure 8A). Next we showed that IRX1 overexpression downregulated *HOXA9* and *HOXA10*, and upregulated target gene *TGFB1*, according to previous studies (Kühn et al., 2016) (Figure 8B). IRX1 overexpression in HEK 293T cells led to a decreased viability and cells lacked the ability to reattach at the flask-surface after they were passaged for a second time, indicating a toxic effect (Figure 8F, supplemental Figure 4). Since HEK 293T viability decreased with IRX1 overexpression, and does not belong to the hematopoietic system, we were still wondering if IRX1 overexpression resulted in lower *HOXA9* expression in OCI AML3 cells as well. Unfortunately, IRX1 did not influence *HOXA9*, but overexpression downregulated *HOXA11* and *TGFB1* in OCI AML3 cells (Figure 8C). However, OCI AML3 cells tolerated IRX1 overexpression, indicating that it was possibly not toxic in hematological cell lines.

H3K27me3 marks on the *HOXA7-11* locus were not influenced by IRX1 overexpression, but the active marks H3K4me3 and H3K27ac were notable decreased (Figure 8D). This could implement that the decreased *HOXA9* expression was mainly caused by reduced active marks rather than an increase in the repressive marker H3K27me3. This result still did not suggest a loss of the TAD boundary, since we would expect that H3K27me3 is transferred across the TAD boundary, resulting in the same epigenetic landscape on both sides.

To investigate the effect of IRX1 overexpression on the TAD boundary, we were also interested in the binding of the CTCF and RAD21 proteins, which are subunits of the cohesion complex (Hill et al., 2016), on different CTCF binding sites (CBS) near the *HOXA9* gene. We found that there was less CTCF present on the TAD boundary between *HOXA10/11* (CBS A10/11), and CTCF levels between the *HOXA7/9* (CBS A7/9) and near *HOXA13* (CBS A13) were not influenced (Figure 8E). Furthermore, RAD21 protein binding seemed slightly reduced at the same CBS A10/11. Interestingly, RAD21 protein levels were increased on the neighboring CBSs. This suggest that loss of the TAD boundary resulted in relocation of the cohesin complex towards a nearby binding site, which was probably independent of the CTCF binding at the same boundary.

It can be concluded that IRX1 overexpression leads to *HOXA9* and *HOXA10* downregulation coinciding with a reduction in active histone marks. Furthermore, it leads to alteration of TAD boundary elements, however the mechanisms are still unknown.

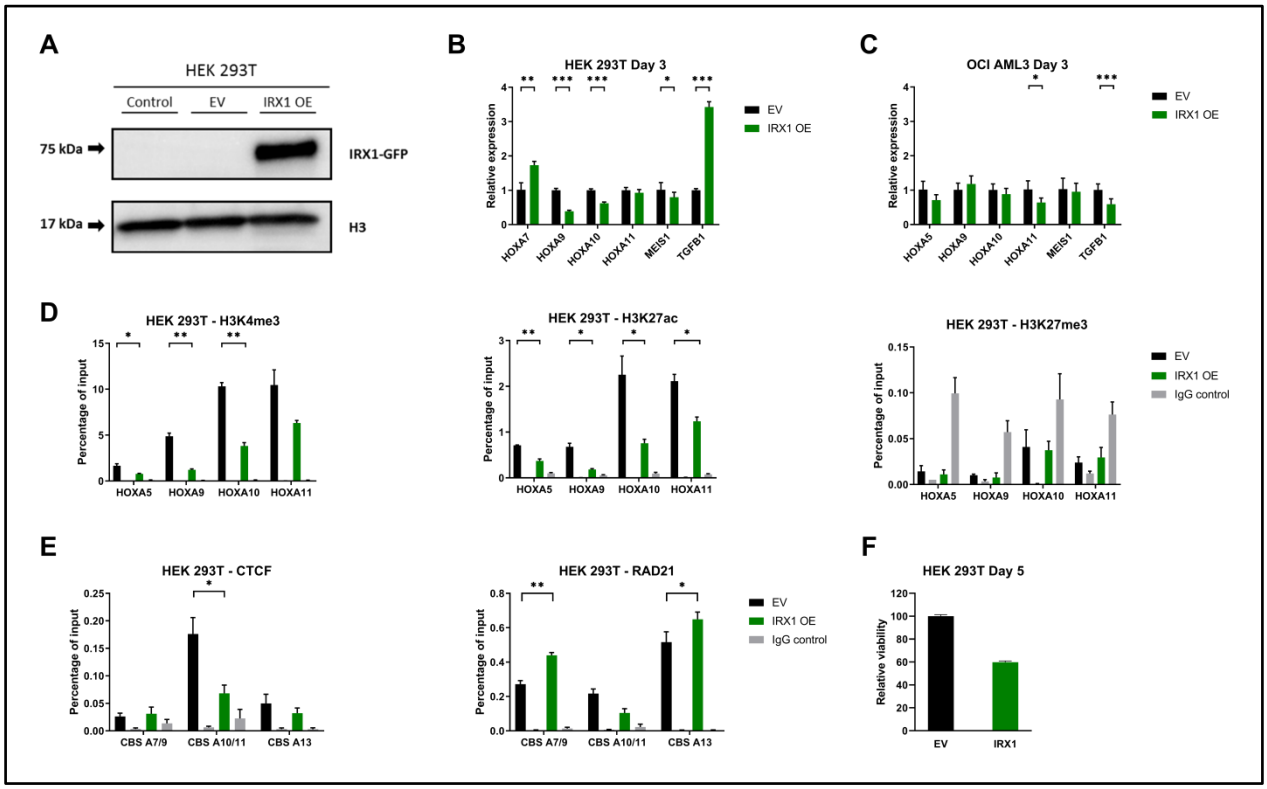


**Figure 8. IRX1 overexpression in HEK 293T cells downregulates HOXA9 and an alters CTCF and RAD21 binding at CBS A10/11.** All data was derived with n = 1. Exact ChIP locations can be found in supplemental figure 3 for H3K4me3, H3K27ac and H3K27me3. ChIP locations for CTCF binding sites can be found in supplemental figure 4. **(A)** Western Blot validation of IRX1-GFP overexpression. **(B)** qPCR results after 3 days of IRX1 overexpression in HEK 293T. *HOXA7-11*, *MEIS1* and *TGFβ1* expression were evaluated. *TGFβ1* is a target gene of IRX1 (Kühn et al., 2016). (**C)** qPCR results after 3 days of IRX1 overexpression in OCI AML3 cells. **(D)** ChIP-qPCR analyses for H3K27me3, H3K4me4, and H3K27ac after 3 days of IRX1 overexpression. **(E)** ChIP-qPCR analyses of CTCF and RAD21 protein levels after 3 days IRX1 overexpression. **(F)** Viability of HEK 293T cells after 5 days of IRX1 overexpression compared to EV transduced HEK 293T cells.

### IRX1 overexpression in CD34$^+$ cells results in impaired cell growth towards the erythroid lineage, but not in accelerated differentiation

Our next step was to test if IRX1 overexpression in sorted CD34$^+$ cells derived from cord blood, would lead to accelerated differentiation, since we suspect that IRX1 overexpression leads to (partly) removal of the TAD boundary based on our results in HEK 293T cells. By forcing CD34$^+$ IRX1 overexpressing cells

into the myeloid, granulocytic, and erythroid lineage by adding cytokines, we suspected to see higher cell surface marker expression at an earlier time point compared to non-transduced $CD34^+$ cells. We analyzed only the GFP-positive fractions of both EV- and IRX1 transduced cells.

Myeloid counts on day 1, 4, 6, 8, and 12 revealed no significant difference between IRX1 overexpressing cells and EV-transduced $CD34^+$ cells (Figure 9A). Furthermore, there was no clear difference in IRX1 or EV viability (supplemental Figure 6A). By analyzing cell surface markers, the MFI of CD15 and CD11b is higher on day 4, 6, and 8, suggesting an accelerated differentiation. There was no difference in the CD114 nor the CD14 MFI. If cells were stimulated towards the granulocytic lineage, there was no difference in cell growth (Figure 9B). Furthermore, analyzing the cell surface markers showed no notable difference compared to the EV, except for the CD11b marker at day 8. IRX1 overexpression in combination with erythroid stimulation resulted in diminished cell growth (Figure 9C). In contrast to the myeloid lineage, IRX1 overexpressing erythroid cells had a lower viability compared to the EV transduced cells. Therefore, we suspected that this was due to more apoptosis. Nevertheless, there was no difference in expression of CD235a or CD71. The GFP positivity remained stable over time in the myeloid lineage, whereas GFP positivity in the granulocytic lineage reduced gradually, and the erythroid GFP positive percentages eventually dropped to less than 5% (supplemental Figure 6A-B). From this experiment, we conclude that IRX1 overexpression did not lead to accelerated differentiation into any lineage.

**Knockdown of *CTCF* in HEK 293T cells increases *HOXA* expression**

Next to our hypothesis that we could remove the TAD boundary with overexpression of myeloid transcription factors, we were also wondering if we could alter the TAD boundary by knocking down the *CTCF* or one of the cohesin genes (*RAD21*, *SMC3*, *SMC1*, and *STAG2*). Another study showed that depletion of a specific CTCF boundary resulted in H3K27me3 spreading towards the *HOXA9* loci, thereby downregulating *HOXA9* expression (Luo, Wang, Zha, Li, Yan, Du, Yang, Sobh, Vulpe, et al., 2018). We hypothesized that if we knocked down *CTCF* in $CD34^+$ cells, it would lead to accelerated $CD34^+$ differentiation into the myeloid lineage by impairing the TAD boundary function (Ouboussad, Kreuz, & Lefevre, 2013).

To validate efficient knockdown, shCTCF-III was introduced to HEK 293T cells. Indeed, CTCF was knocked down by 80% compared to the scrambled control shSCR (Figure 10B). Since CTCF and the cohesin complex usually binds at TAD boundaries, we would suspect that knockdown of *CTCF* would affect the expression of cohesin genes *RAD21*, *SMC1A*, *SMC3*, or *STAG2*. Of these cohesin genes, RAD21 was affected and upregulated a 2-fold, and SMC1A was slightly increased after 4 days of *CTCF* KD (Figure 10C), suggesting that loss of CTCF is compensated by an increased expression of other cohesin genes. Furthermore, since our original hypothesis would implicate a downregulation of HOXA9 expression after TAD boundary alteration, we analyzed the effect of *CTCF* KD on *HOXA* genes. Interestingly, all measured *HOXA* genes were highly upregulated (5- to 13 times) (Figure 10D). Since this is contradictory to our thoughts, we performed a ChIP for CTCF and RAD21 to check the binding of cohesin to the CTCF binding sites (CBS). As expected, CTCF binding was reduced at the CBS A10/11, but more remarkable was that RAD21 binding was not decreased upon loss of CTCF at CBS A10/11. RAD21 was slightly enhanced at CBS A7/9, similar to our results in IRX1 overexpressed HEK 293T cells (Figure 10E). To determine if *HOXA* upregulation upon *CTCF* KD was due to enhanced active markers, we performed a ChIP for H3K4me3 or H3K27ac as well. H3K4me3 was slightly enhanced on the *HOXA9* and *HOXA10* loci, which corresponds with enhanced H3K27ac at *HOXA10*. On the contrary, H3K27ac marks were reduced on *HOXA5* and *HOXA11*.

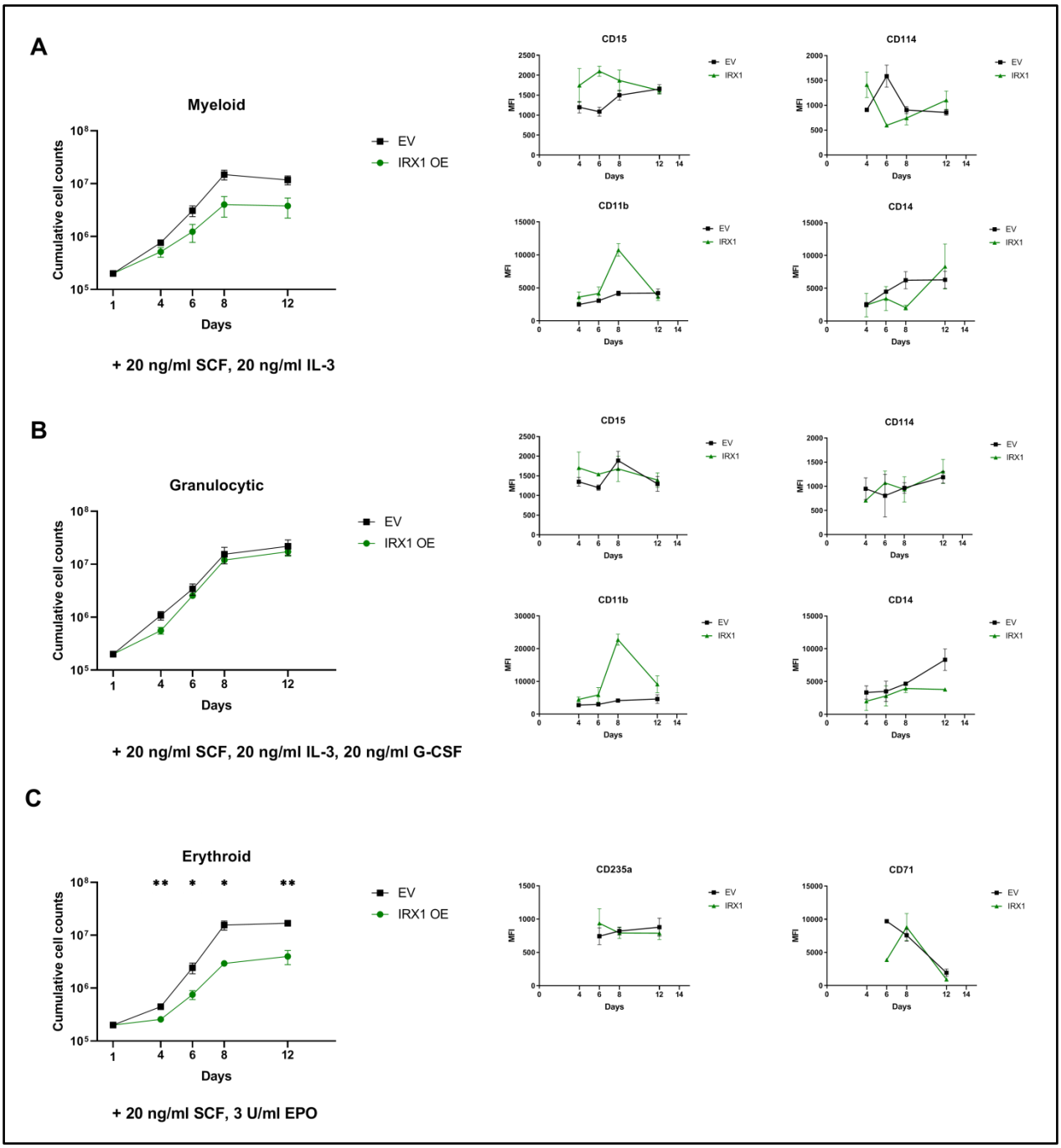


**Figure 9. IRX1 overexpression in CD34⁺ cells results in impaired cell growth when stimulated into the erythroid compartment, but not in accelerated differentiation.** CD34⁺ cells were isolated from cord blood, and transduced with IRX1-GFP and EV-GFP. Cell surface markers analysis is representative for the GFP positive fraction. All data was derived with n = 3. **(A)** CD34⁺ cumulative cell count towards the myeloid lineage, supplemented with the MFI of CD15, CD114, CD11b, and CD14. **(B)** CD34⁺ cumulative cell count towards the granulocytic lineage, supplemented with the MFI of CD15, CD114, CD11b, and CD14. **(C)** CD34⁺ cumulative cell count towards the erythroid lineage, supplemented with the MFI of CD235a and CD71.

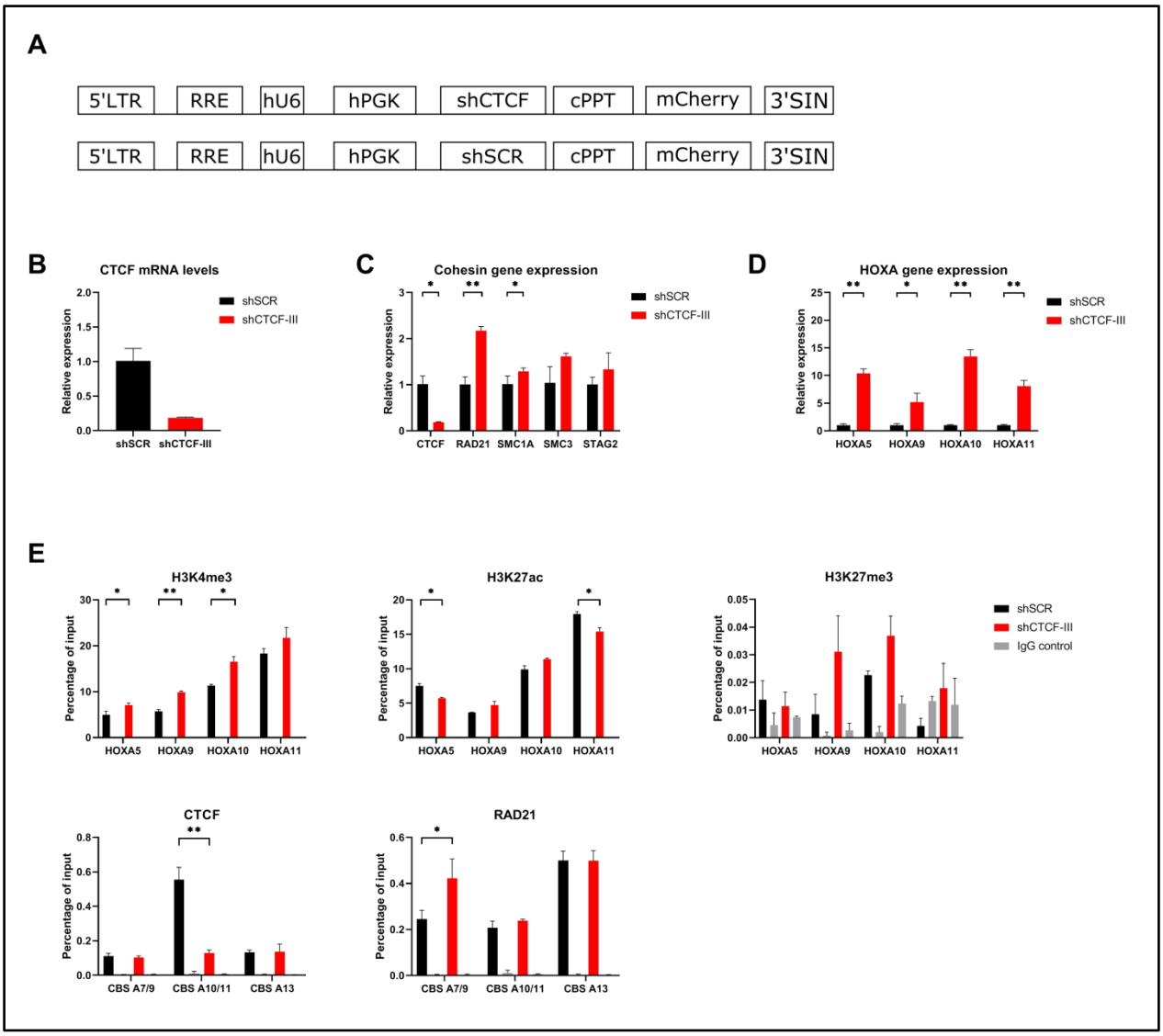


**Figure 10. KD of *CTCF* in HEK 293T results in upregulation of *HOXA* genes and enhanced H3K4me3 marks.** All data was derived with n = 1. (A) Schematical representation of the lentiviral shCTCF-III and shSCR constructs used in this experiment. **(B)** KD confirmation by qPCR for CTCF expression compared to the control shSCR. mRNA was isolated 4 days post transduction. **(C)** qPCR for cohesin genes (*RAD21*, *SMC1A*, *SMC3*, and *STAG2*) of HEK 293T cells on day 4 with shCTCF-III. **(D)** qPCR for *HOXA* genes of HEK 293T cells on day 4 with shCTCF-III. **(E)** 8 x $10^6$ HEK 293T cells were cross-linked for ChIP for both control (shSCR) and shCTCF-III. Antibodies for H3K27me3, H3K4me4, H3K27ac, CTCF, and RAD21 were used, and purified DNA was analyzed by qPCR for *HOXA* loci and CTCF binding sites.

## Discussion

We hypothesized that overexpression or reintroduction of transcription factors (CEBPa, PU.1, and IRX1) resulted in a TAD boundary depletion on the *HOXA* locus, thereby repressing *HOXA* genes and reinitiating differentiation towards the myeloid lineage. There was an TAD boundary present in healthy cord blood $CD34^{+}$ cells and in $NPM1^{cyt}$ AML patients on the CTCF binding site (CBS) between *HOXA10* and *HOXA11*, which was lost upon myeloid differentiation and also in $NPM1^{wt}$ AML patients (van den Boom et al., 2016; Yi et al., 2019). $NPM1^{cyt}$ AML patients were furthermore associated with a decreased *IRX1* expression and upregulated *HOXA9* expression (Alcalay et al., 2005; Haferlach et al., 2010; Kohlmann et al., 2008; Rapin et al., 2014; Svendsen et al., 2016). Therefore, we studied the effect of these TFs in $NPM1^{cyt}$ leukemic cell lines, and OCI AML3 in particular.

In order to study whether the transcription factor CEBPa would alter the TAD boundary, OCI AML3 cells were transduced with an inducible CEBPa-ER system (Wierenga et al., 2010). It has been shown that CEBPa overexpression resulted in downregulated *HOXA9* expression in multiple AML cell lines, although not in OCI AML3 cells yet (Loke et al., 2018; Matsushita et al., 2008). CEBPa overexpression in OCI AML3 cells did not result in altered *HOXA* expression as we expected. This could be explained by that the used cell lines (e.g. Kasumi-1) in the previous mentioned studies did not harbor the $NPM1^{mut}$, as the OCI AML3 cells do. Furthermore, Loke *et al.* (2018) mentioned that CEBPa overexpression reduces the maintenance of leukemia in a cell-type specific way. This, combined with our conclusion that CEBPa did not alter *HOXA* expression, could explain why there were no (epi)genetic changes on the *HOXA* locus, although the MFI of myeloid cell-surface markers was higher after CEBPa overexpression. A higher MFI in combination with upregulated SIRPa expression can indicate that the cells were slightly more myeloid committed. However, the cell morphology was not changed after 10 days, suggesting that there was another regulator that blocked myeloid differentiation. Moreover, Loke *et al.* (2018) stated that overexpression of CEBPa did not result in removal of leukemic fusion-proteins from their binding site, but that it overrides their repressive function. Given the above, it is possible that CEBPa was not highly upregulated to induce *HOXA* changes, suggesting a dose-dependent role for CEBPa, which is also reported for PU.1 (Burda et al., 2009). Therefore, it can be of interest to repeat the experiment with different doses of 4-OHT, and check if higher doses of 4-OHT lead to altered *HOXA* expression. Additionally, due to the $NPM1^{cyt}$ in OCI AML3, PU.1 is predominantly localized in the cells cytoplasm instead of the nucleus. CEBPa and PU.1 have separate independent functions, but since they can also cooperate, and CEBPa functions are impaired in the absence of PU.1 (Sive et al., 2016), it is possible that CEBPa overexpression alone in OCI AML3 cells is not sufficient to induce changes of *HOXA* genes or differentiation. This suggests that overexpression of CEBPa in combination with relocation or overexpression of PU.1 could result in altered *HOXA* expression in OCI AML3 cells and initiate differentiation. However, blocking of the nuclear export gene (*XPO1*) resulted in that PU.1 could not leave the cell's nucleus, resulting in differentiation of AML cells (Gu et al., 2018), suggesting that PU.1 relocation alone would be sufficient enough to initiate differentiation without CEBPa overexpression. Despite the fact that these experiments were done in OCI AML3, which lacked the TAD boundary between *HOXA10* and *HOXA11*, this is not the most promising transcription factor (TF) to continue. Due to these results and time limits, we decided that we would not continue working with CEBPa, though it is interesting to study what the reason is of the differentiation block in OCI AML3 cells.

PU.1 was another potential candidate to alter TAD boundaries when overexpressed. We concluded that PU.1 overexpression did not lead to changes in *HOXA* expression, in contrast to other studies (Gu et al., 2018). In the study of Gu *et al.* (2018), PU.1 overexpression studies were performed in HEK293 cells with no mutant *NPM1*. In $NPM1^{cyt}$ cells, $NPM1^{cyt}$ interacts with PU.1 and is responsible for delocalization of PU.1 towards the cytoplasm. In our inducible system, the PU.1-ER goes to the nucleus

after induction with 4-OHT. It is possible that the NPM1$^{cyt}$ interacts with the PU.1-ER as well and that it is responsible for transport towards the cytoplasm, thereby abolishing the PU.1 overexpression. This NPM1$^{cyt}$ related export is initiated by *XPO1* (Falini et al., 2006), and inhibiting XPO1 with selinexor has already been proven to induce differentiation again (Gu et al., 2018). Nevertheless, PU.1 overexpression in HEK 293T cells did not show altered *HOXA* genes in contrast to the previously mentioned study.

We were most intrigued by the fact that the OCI AML3 cell line did not have the TAD boundary as we had observed in NPM1$^{cyt}$ AML patients (Figure 7A). Analyzing data sets of Brunetti *et al.* (2018) explained why we did not observed the presence of H3K27me3 in OCI AML3 cells since the complete *HOXA* locus lacks this repressive mark. If this OCI AML3 cell line would have had the same epigenetic landscape, we suspected H3K27me3 transfer to the *HOXA9* locus, where it was initially not present, from the other side of the TAD boundary. Therefore, our first thoughts on the lack of H3K27me3 were that both CEBPa and PU.1 overexpression did not altered the TAD boundary. Given the above, we actually only can conclude that CEBPa or PU.1 overexpression did not alter *HOXA* expression, but we cannot answer our hypothesis if they alter TAD boundaries, because OCI AML3 cells does not have a TAD boundary where we expected it to be. Therefore we focused on wrong marks, maybe H3K9me3 was a better indicator, and on the wrong loci, *HOXA5* and *HOXA6* would have been potential loci. Due to time limits, we then only focused on the IRX1 overexpression, instead of analyzing CEBPa overexpression in HEK 293T cells. We did a quick experiment with PU.1 overexpression in these cells, but that did not resulted in altered *HOXA* expression (Figure 6D).

Overexpression of IRX1 in HEK 293T cells resulted in downregulation of *HOXA9* and *HOXA10*, as was shown previously (A. Kühn et al., 2016). We hypothesized that this downregulation would be due to H3K27me3 transfer towards the active *HOXA9* TAD, however the *HOXA9* downregulation was probably due to the downregulation of active markers H3K4me3 and H3K27me3. To see if TAD boundaries were altered, we checked CTCF and RAD21 protein binding at different CTCF binding sites on the *HOXA* locus. Since CTCF sites are associated with the cohesin complex (Dixon et al., 2012), RAD21 levels were checked as indicator for the cohesin complex. Lowered protein binding indicates that the TAD boundary indeed was altered. Interestingly, it seemed as if RAD21 had spread from the CBS A10/11 towards the nearby CBS A7/9. In order to state that the whole cohesin complex moves towards nearby CBS, future experiments can be done with ChIP antibodies for SMC1A, SMC3 and STAG2. Moving the cohesin complex, and thereby a (sub)TAD, from CBS A10/11 towards CBS A7/9 could clarify why *HOXA7* is upregulated after IRX1 overexpression, although that is contradictory to other studies (A. Kühn et al., 2016). Since the TAD boundary is altered, but H3K27me3 levels are not affected and H3K4me3 is downregulated, it can be suggested that multiple histone demethylases (HMTs) are repressed or activated, like KDM2B or KDM6A/B (Agger et al., 2007; Frescas et al., 2007). However, in the study of A. Kühn *et al.* (2016), only JMJD1C comes forward as a downregulated histone demethylase, which is responsible for H3K9 methylation (Chen et al., 2015), and none of the other HMTs. Interestingly, JMJD1C is in fact a coactivator of TFs and mediator of AML, since it directly interacts with *HOXA9* expression (Zhu et al., 2016). In that particular study, JMJD1C depletion did not result in clear differences of H3K4me3 or H3K27me3, while we see a clear drop of H3K4me3 levels, indicating a different pathway.

Unfortunately, we were only able to overexpress IRX1 in two TAD boundary associated cells, namely HEK 293T and healthy cord blood CD34$^{+}$ cells. It is interesting to do experiments with IRX1 overexpression in other AML cell lines known for an intact TAD boundary, to see if it can alter TAD boundaries there as well, and if that would result in reinitiating differentiation. Our CD34$^{+}$ experiment was unfortunately unsorted, so we could not take a decent insight into the genetics of *HOXA* or cohesin genes. Despite the unsorted experiment, transduced CD34$^{+}$ cells with IRX1 showed an impaired growth towards the myeloid and granulocytic lineage. However, cell viability was not affected after 14 days, suggesting that IRX1 could play a role in cell proliferation. This is also supported by slowly decreasing GFP percentages compared to the GFP negative fraction. Sorting CD34$^{+}$ cells after transduction was not yet

successful due to low viability after transduction, probably caused by an abundance of Polybrene addition (8 µg/µl instead of 2-4 µg/µl). For an upcoming experiment we would suggest to sort cells after transduction, follow them during differentiation, and analyze the cells every 2 days for *HOXA* and cohesin expression, and cell surface markers.

During differentiation, TAD structures also display alterations, thereby altering the interactions between genes (Boya et al., 2017). This indicates that the reorganization of chromatin can play a role in a cell- and lineage-specific transcription pattern, which determines the cells commitment. Therefore, we hypothesized that we could alter the TAD boundary by KD of *CTCF*, *RAD21*, *SMC3*, *SMC1A*, or *STAG2*, and that it would result in a depletion of the TAD boundary, thereby repressing *HOXA9* and initiating a myeloid differentiation. We were only able to transduce HEK 293T cells with one shRNA for *CTCF* (shCTCF-III), and none with a shRNA for the cohesin genes. KD of CTCF in CMPs resulted in acceleration of myeloid differentiation, however, they did not studied the effect on the *HOXA* locus (Ouboussad et al., 2013). CTCF depletion in hematopoietic stem and progenitor cells (HSCPCs) did not result in altered *HOXA* expression (Fisher et al., 2017), although the cell viability decreased in accordance with our results. In CMPs, there was no difference in apoptosis or cell growth compared to the control. Furthermore, depletion of the specific CBS between *HOXA7* and *HOXA9*, resulted in reinitiated differentiation by the removal of the TAD boundary and thereby the transfer of H3K27me3 to the neighboring TAD (Luo et al., 2018). Consequently, would suspect that CTCF KD would lead to a 'leaky' TAD boundary, since CTCF is required for the cohesin complex to bind to the proper sites onto the DNA (Wendt et al., 2008), thereby forming the TAD boundary. However, CTCF is not required to load the cohesin complex onto DNA, which is supported by our data that RAD21 protein binding is not altered at CTCF binding sites at CBS A10/11 and CBS A13. The other way around, the cohesin complex is necessary for the insulator function of CTCF, however we were not able to test this (Wendt et al., 2008). Interestingly, cohesin KD is known to initiate myeloid disorders by enhancing the self-renewal of HSCs both *in vitro* as *in vivo* (Galeev et al., 2016; Mazumdar et al., 2015). Interestingly, after CTCF KD, *HOXA* genes are remarkably upregulated. This effect is similar to RAD21 KD, which is proposed to be initiated by PRC2 activation, since RAD21 is responsible for PRC2 silencing in normal conditions (Fisher et al., 2017). The PRC2 complex is also regulated by CTCF in the same way as RAD21 which supports our result of upregulated HOXA genes after CTCF KD (Xu et al., 2014). However, H3K27me3 levels are not downregulated in our study, so the role of the PRC2 complex in this context remains unknown and additional studies are required. The lack of H3K27me3 spreading after CTCF KD was also seen in other studies, including the deletion of a single CTCF site within the *HOXA* locus (Narendra et al., 2016; Narendra et al., 2015; Nora et al., 2017). These results actually challenge the idea that CTCF prevents directly heterochromatin spreading by acting as a "roadblock" (Alipour & Marko, 2012). Furthermore, it is indicated that TAD compartments are preserved without CTCF, although loop extrusion proceeds beyond the TAD boundary. Nevertheless, CTCF is necessary for stable loop extrusions, and complete depletion of CTCF in Drosophila and mice results in lethality (Gambetta & Furlong, 2018; Moore et al., 2012). Recently, it was shown that *Stag2* depletion in mice resulted in enhanced stem cell function and an altered the lineage commitment of cells. Furthermore, since *Stag1* was able to bind at some TAD boundaries that were previously bound by *Stag2*, the occupancy of CTCF, Smc1a, and Smc3 at these boundaries were mainly not altered. This indicated that the role *Stag2* in hematopoiesis and gene regulation was independent of CTCF. Furthermore, reactivation of target genes of *Stag2* like *Ebf1* and *Pax5* reversed the altered stem cell function and restored differentiation. Interestingly, PU.1 restoration in *Stag2*$^{-/-}$ did not rescue the impact of the depletion. Since PU.1 was one of our target TFs to alter TAD boundaries, it could implicate that this is a reason why there was no effect after overexpression. It can be of interest to target *EBF1* and *PAX5* or other target genes in AML cells with a cohesin mutation or induced KD to see the effect on TAD boundaries and differentiation. In addition, since cohesin gene KD and CTCF KD results in altered phenotypes of cells, and sometimes even proved to be lethal, a more

subtle approach like Crispr-Cas9 would be favorable for future research on the effect CTCF or cohesin genes on TAD boundary.

Altogether, we conclude that PU.1 overexpression does not alter *HOXA* gene expression in OCI AML3 cells. Due to the different TAD boundary location in those cells compared to AML patients with an intact TAD boundary, we looked into wrong loci, thereby we cannot conclude if CEBPa or PU.1 alters TAD boundaries. IRX1 is a potential regulator of TAD boundaries since overexpression resulted in lowered CTCF and RAD21 protein binding at the CTCF A10/11 site, and downregulation of *HOXA9* expression. However, this exact mechanism has to be unraveled in future research.

## References


Agger, K., Cloos, P. A. C., Christensen, J., Pasini, D., Rose, S., Rappsilber, J., … Helin, K. (2007). UTX and JMJD3 are histone H3K27 demethylases involved in HOX gene regulation and development. *Nature*, *449*(7163), 731–734. https://doi.org/10.1038/nature06145

Alcalay, M., Tiacci, E., Bergomas, R., Bigerna, B., Venturini, E., Minardi, S. P., … Pelicci, P. G. (2005). Acute myeloid leukemia bearing cytoplasmic nucleophosmin (NPMc+ AML) shows a distinct gene expression profile characterized by up-regulation of genes involved in stem-cell maintenance. *Blood*, *106*(3), 899–902. https://doi.org/10.1182/blood-2005-02-0560

Alharbi, R. A., Pettengell, R., Pandha, H. S., & Morgan, R. (2013). The role of HOX genes in normal hematopoiesis and acute leukemia. *Leukemia*, *27*(5), 1000–1008. https://doi.org/10.1038/leu.2012.356

Alipour, E., & Marko, J. F. (2012). Self-organization of domain structures by DNA-loop-extruding enzymes. *Nucleic Acids Research*, *40*(22), 11202–11212. https://doi.org/10.1093/nar/gks925

Benveniste, P., Frelin, C., Janmohamed, S., Barbara, M., Herrington, R., Hyam, D., & Iscove, N. N. (2010). Intermediate-Term Hematopoietic Stem Cells with Extended but Time-Limited Reconstitution Potential. *Cell Stem Cell*, *6*(1), 48–58. https://doi.org/10.1016/j.stem.2009.11.014

Birbrair, A., & Frenette, P. S. (2017). Niche heterogeneity in the bone marrow. *Ann N Y Acad Sci.*, *1370*(1), 82–96. https://doi.org/10.1111/nyas.13016.Niche

Boisset, J. C., & Robin, C. (2012). On the origin of hematopoietic stem cells: Progress and controversy. *Stem Cell Research*, *8*(1), 1–13. https://doi.org/10.1016/j.scr.2011.07.002

Boya, R., Yadavalli, A. D., Nikhat, S., Kurukuti, S., Palakodeti, D., & Pongubala, J. M. R. (2017). Developmentally regulated higher-order chromatin interactions orchestrate B cell fate commitment. *Nucleic Acids Research*, *45*(19), 11070–11087. https://doi.org/10.1093/nar/gkx722

Bradford, G. B., Williams, B., Rossi, R., & Bertoncello, I. (1997). Quiescence, cycling, and turnover in the primitive hematopoietic stem cell compartment. *Experimental Hematology*, *25*(5), 445—453. Retrieved from http://europepmc.org/abstract/MED/9168066

Brunetti, L., Gundry, M. C., Sorcini, D., Martelli, M. P., Falini, B., & Goodell, M. A. (2018). Mutant NPM1 Maintains the Leukemic State through HOX Expression. *Cancer Cell*, *34*(3), 499-512.e9. https://doi.org/10.1016/j.ccell.2018.08.005

Burda, P., Curik, N., Kokavec, J., Basova, P., Mikulenkova, D., Skoultchi, A. I., … Stopka, T. (2009). PU.1 activation relieves GATA-1-mediated repression of Cebpa and Cbfb during leukemia differentiation. *Molecular Cancer Research*, *7*(10), 1693–1703. https://doi.org/10.1158/1541-7786.MCR-09-0031

Buske, C., Feuring-Buske, M., Abramovich, C., Spiekermann, K., Eaves, C. J., Coulombel, L., … Humphries, R. K. (2002). Deregulated expression ofHOXB4 enhances the primitive growth activity ofhuman hematopoietic cells. *Blood*, *100*(3), 862–868.

Camós, M., Esteve, J., Jares, P., Colomer, D., Rozman, M., Villamor, N., … Campo, E. (2006). Gene expression profiling of acute myeloid leukemia with translocation t(8;16)(p11;p13) and MYST3-CREBBP rearrangement reveals a distinctive signature with a specific pattern of HOX gene expression. *Cancer Research*, *66*(14), 6947–6954. https://doi.org/10.1158/0008-5472.CAN-05-4601

Cancer Genome Atlas Research Network. (2013). Genomic and Epigenomic Landscapes of Adult De Novo Acute Myeloid Leukemia. *New England Journal of Medicine*, *368*(22), 2059–2074. https://doi.org/10.1056/NEJMoa1301689

Chen, M., Zhu, N., Liu, X., Laurent, B., Tang, Z., Eng, R., … Roeder, R. G. (2015). JMJD1C is required for the survival of acute myeloid leukemia by functioning as a coactivator for key transcription factors. *Genes and Development*, *29*(20), 2123–2139. https://doi.org/10.1101/gad.267278.115

Collins, C. T., & Hess, J. L. (2016). Deregulation of the HOXA9 / MEIS1 axis in acute leukemia. *Current Opinion in Hematology*, *23*(4), 354–361. https://doi.org/10.1097/MOH.0000000000000245

Collins, C., Wang, J., Miao, H., Bronstein, J., Nawer, H., Xu, T., … Hess, J. L. (2014). CEBPα is an essential collaborator in HOXA9/MEIS1-mediated leukemogenesis. *PNAS*, *111*(27), 9899–9904.

Corces-Zimmerman, M. R., Hong, W. J., Weissman, I. L., Medeiros, B. C., & Majeti, R. (2014). Preleukemic mutations in human acute myeloid leukemia affect epigenetic regulators and persist in remission. *Proceedings of the National Academy of Sciences of the United States of America*, *111*(7), 2548–2553.

https://doi.org/10.1073/pnas.1324297111
Cremer, T., & Cremer, C. (2001). Chromosome territories, nuclear architecture and gene regulation in mammalian cells. *Nature Reviews Genetics*. https://doi.org/10.1038/35066075
Cubeñas-Potts, C., & Corces, V. G. (2015). Architectural proteins, transcription, and the three-dimensional organization of the genome. *FEBS Letters*, *589*(20), 2923–2930. https://doi.org/10.1016/j.febslet.2015.05.025
Ding, L., Ley, T. J., Larson, D. E., Miller, C. A., Koboldt, D. C., Welch, J. S., … Dipersio, J. F. (2012). Clonal evolution in relapsed acute myeloid leukaemia revealed by whole-genome sequencing. *Nature*, *481*(7382), 506–510. https://doi.org/10.1038/nature10738
Dixon, J. R., Hu, M., Ren, B., Li, Y., Liu, J. S., Kim, A., … Shen, Y. (2012). Topological domains in mammalian genomes identified by analysis of chromatin interactions. *Nature*, *485*(7398), 376–380. https://doi.org/10.1038/nature11082
Faber, J., Krivtsov, A. V., Stubbs, M. C., Wright, R., Davis, T. N., Van Heuvel-Eibrink, M. Den, … Armstrong, S. A. (2009). HOXA9 is required for survival in human MLL-rearranged acute leukemias. *Blood*, *113*(11), 2375–2385. https://doi.org/10.1182/blood-2007-09-113597
Falini, B., Bolli, N., Liso, A., Martelli, M. P., Mannucci, R., Pileri, S., & Nicoletti, I. (2009). Altered nucleophosmin transport in acute myeloid leukaemia with mutated NPM1: Molecular basis and clinical implications. *Leukemia*, *23*(10), 1731–1743. https://doi.org/10.1038/leu.2009.124
Falini, B., Shan, J., Martelli, M. P., Liso, A., Pucciarini, A., Bigerna, B., … Martelli, M. F. (2006). Both carboxy-terminus NES motif and mutated tryptophan(s) are crucial for aberrant nuclear export of nucleophosmin leukemic mutants in NPMc+ AML. *Blood*, *107*(11), 4514–4523. https://doi.org/10.1182/blood-2005-11-4745.Supported
Fisher, J. B., Peterson, J., Reimer, M., Stelloh, C., Pulakanti, K., Gerbec, Z. J., … Rao, S. (2017). The cohesin subunit Rad21 is a negative regulator of hematopoietic self-renewal through epigenetic repression of Hoxa7 and Hoxa9. *Leukemia*. https://doi.org/10.1038/leu.2016.240
Frank, S. R., Schroeder, M., Fernandez, P., Taubert, S., & Amati, B. (2001). Binding of c-Myc to chromatin mediates mitogen-induced acetylation of histone H4 and gene activation. *Genes and Development*, *15*(16), 2069–2082. https://doi.org/10.1101/gad.906601
Frescas, D., Guardavaccaro, D., Bassermann, F., Koyama-Nasu, R., & Pagano, M. (2007). JHDM1B/FBXL10 is a nucleolar protein that represses transcription of ribosomal RNA genes. *Nature*, *450*(7167), 309–313. https://doi.org/10.1038/nature06255
Galeev, R., Baudet, A., Kumar, P., Rundberg Nilsson, A., Nilsson, B., Soneji, S., … Larsson, J. (2016). Genome-wide RNAi Screen Identifies Cohesin Genes as Modifiers of Renewal and Differentiation in Human HSCs. *Cell Reports*, *14*(12), 2988–3000. https://doi.org/10.1016/j.celrep.2016.02.082
Gambetta, M. C., & Furlong, E. E. M. (2018). The insulator protein CTCF is required for correct hox gene expression, but not for embryonic development in Drosophila. *Genetics*, *210*(1), 129–136. https://doi.org/10.1534/genetics.118.301350
Gentile, C., & Kmita, M. (2018). The remote transcriptional control of Hox genes, *692*, 685–692. https://doi.org/10.1387/ijdb.180198mk
Golub, T. R., Slonim, D. K., Tamayo, P., Huard, C., Gaasenbeek, M., Mesirov, J. P., … Lander, E. S. (1999). Molecular classification of cancer: Class discovery and class prediction by gene expression monitoring. *Science*, *286*(5439), 531–527. https://doi.org/10.1126/science.286.5439.531
Gu, X., Jha, B. K., Saunthararajah, Y., Gu, X., Ebrahem, Q., Mahfouz, R. Z., … Landesman, Y. (2018). Leukemogenic nucleophosmin mutation disrupts the transcription factor hub that regulates granulomonocytic fates. *The Journal of Clinical Investigation*, *128*(10), 4260–4279.
Guelen, L., Pagie, L., Brasset, E., Meuleman, W., Faza, M. B., Talhout, W., … Van Steensel, B. (2008). Domain organization of human chromosomes revealed by mapping of nuclear lamina interactions. *Nature*, *453*(7197), 948–951. https://doi.org/10.1038/nature06947
Haferlach, T., Kohlmann, A., Wieczorek, L., Basso, G., Te Kronnie, G., Béné, M. C., … Foà, R. (2010). Clinical utility of microarray-based gene expression profiling in the diagnosis and subclassification of leukemia: Report from the international microarray innovations in leukemia study group. *Journal of Clinical Oncology*, *28*(15), 2529–2537. https://doi.org/10.1200/JCO.2009.23.4732
Henkel, G. W., McKercher, S. R., Leenen, P. J. M., & Maki, R. A. (1999). Commitment to the monocytic lineage occurs in the absence of the transcription factor PU.1. *Blood*, *93*(9), 2849–2858.
Hill, V. K., Kim, J. S., & Waldman, T. (2016). Cohesin mutations in human cancer. *Biochimica et Biophysica Acta* -

*Reviews on Cancer*, *1866*(1), 1–11. https://doi.org/10.1016/j.bbcan.2016.05.002

Hohaus, S., Petrovick, M. S., Voso, M. T., Sun, Z., Zhang, D. E., & Tenen, D. G. (1995). PU.1 (Spi-1) and C/EBP alpha regulate expression of the granulocyte-macrophage colony-stimulating factor receptor alpha gene. *Molecular and Cellular Biology*, *15*(10), 5830–5845. https://doi.org/10.1128/mcb.15.10.5830

Hu, Z., Gu, X., Baraoidan, K., Ibanez, V., Sharma, A., Kadkol, S. H., … Saunthararajah, Y. (2011). RUNX1 regulates corepressor interactions of PU.1. *Blood*, *117*(24), 6498–6508. https://doi.org/10.1182/blood-2010-10-312512

Iwasaki, H., Somoza, C., Shigematsu, H., Duprez, E. A., Iwasaki-Arai, J., Mizuno, S., … Akashi, K. (2005). Distinctive and indispensable roles of PU.1 in maintenance of hematopoietic stem cells and their differentiation. *Blood*, *106*(5), 1590–1600. https://doi.org/10.1182/blood-2005-03-0860.Supported

Kester, L., & van Oudenaarden, A. (2018). Single-Cell Transcriptomics Meets Lineage Tracing. *Cell Stem Cell*, *23*(2), 166–179. https://doi.org/10.1016/j.stem.2018.04.014

Knapp, D. J. H. F., Hammond, C. A., Hui, T., Van Loenhout, M. T. J., Wang, F., Aghaeepour, N., … Eaves, C. J. (2018). Single-cell analysis identifies a CD33 + subset of human cord blood cells with high regenerative potential. *Nature Cell Biology*, *20*(6), 710–720. https://doi.org/10.1038/s41556-018-0104-5

Kohlmann, A., Kipps, T. J., Rassenti, L. Z., Downing, J. R., Shurtleff, S. A., Mills, K. I., … Haferlach, T. (2008). An international standardization programme towards the application of gene expression profiling in routine leukaemia diagnostics: The Microarray Innovations in LEukemia study prephase. *British Journal of Haematology*, *142*(5), 802–807. https://doi.org/10.1111/j.1365-2141.2008.07261.x

Kon, A., Shih, L. Y., Minamino, M., Sanada, M., Shiraishi, Y., Nagata, Y., … Ogawa, S. (2013). Recurrent mutations in multiple components of the cohesin complex in myeloid neoplasms. *Nature Genetics*, *45*(10), 1232–1237. https://doi.org/10.1038/ng.2731

Korthuis, P. M., Berger, G., Bakker, B., Rozenveld-Geugien, M., Jaques, J., De Haan, G., … Schepers, H. (2015). CITED2-mediated human hematopoietic stem cell maintenance is critical for acute myeloid leukemia. *Leukemia*. https://doi.org/10.1038/leu.2014.259

Krumlauf, R. (1994). Hox genes in vertebrate development. *Cell*. https://doi.org/10.1016/0092-8674(94)90290-9

Kühn, A., Löscher, D., & Marschalek, R. (2016). The IRX1/HOXA connection: insights into a novel t(4;11)- specific cancer mechanism. *Oncotarget*, *7*(23), 35341–35352. https://doi.org/10.18632/oncotarget.9241

Kühn, M. W. M., Song, E., Feng, Z., Sinha, A., Chen, C. W., Deshpande, A. J., … Armstrong, S. A. (2016). Targeting chromatin regulators inhibits leukemogenic gene expression in NPM1 mutant leukemia. *Cancer Discovery*, *6*(10), 1166–1181. https://doi.org/10.1158/2159-8290.CD-16-0237

Lasa, A., Carnicer, M. J., Aventín, A., Estivill, C., Brunet, S., Sierra, J., & Nomdedéu, J. F. (2004). MEIS 1 expression is downregulated through promoter hypermethylation in AML1-ETO acute myeloid leukemias. *Leukemia*, *18*(7), 1231–1237. https://doi.org/10.1038/sj.leu.2403377

Lawrence, H. J., Helgason, C. D., Sauvageau, G., Fong, S., Izon, D. J., Humphries, R. K., & Largman, C. (1997). Mice bearing a targeted interruption of the homeobox gene HOXA9 have defects in myeloid, erythroid, and lymphoid hematopoiesis. *Blood*, *89*(6), 1922–1930.

Lawrence, H. J., & Largman, C. (1992). Homeobox Genes in Normal Hematopoiesis and Leukemia By. *Journal of American Society of Hematology*, *80*, 2445–2453.

Lawrence, H. J., Rozenfeld, S., Cruz, C., Matsukuma, K., Kwong, A., Kömüves, L., … Largman, C. (1999). Frequent co-expression of the HOXA9 and MEIS1 homeobox genes in human myeloid leukemias. *Leukemia*, *13*(12), 1993–1999. https://doi.org/10.1038/sj.leu.2401578

Lieberman-aiden, E., Berkum, N. L. Van, Williams, L., Imakaev, M., Ragoczy, T., Telling, A., … Mirny, L. A. (2009). Comprehensive Mapping of Long-Range Interactions Reveals Folding Principles of the Human Genome. *Science*, *326*, 289–293.

Lin, L. I., Chen, C. Y., Lin, D. T., Tsay, W., Tang, J. L., Yeh, Y. C., … Tien, H. F. (2005). Characterization of CEBPA mutations in acute myeloid leukemia: Most patients with CEBPA mutations have biallelic mutations and show a distinct immunophenotype of the leukemic cells. *Clinical Cancer Research*, *11*(4), 1372–1379. https://doi.org/10.1158/1078-0432.CCR-04-1816

Loke, J., Chin, P. S., Keane, P., Pickin, A., Assi, S. A., Ptasinska, A., … Bonifer, C. (2018). C/EBPa overrides epigenetic reprogramming by oncogenic transcription factors in acute myeloid leukemia. *Blood Advances*, *2*(3), 271–284.

Luo, H., Wang, F., Zha, J., Li, H., Yan, B., Du, Q., … Huang, S. (2018). CTCF boundary remodels chromatin domain and drives aberrant HOXgene transcription in acute myeloid leukemia. *Blood*, *132*(8), 837–848.

Luo, H., Wang, F., Zha, J., Li, H., Yan, B., Du, Q., … Vulpe, C. (2018). CTCF boundary remodels chromatin domain and

drives aberrant HOX gene transcription in acute myeloid leukemia, *132*(8), 837–849. https://doi.org/10.1182/blood-2017-11-814319

Macaulay, I. C., Svensson, V., Labalette, C., Ferreira, L., Hamey, F., Voet, T., … Cvejic, A. (2016). Single-Cell RNA-Sequencing Reveals a Continuous Spectrum of Differentiation in Hematopoietic Cells. *Cell Reports*, *14*(4), 966–977. https://doi.org/10.1016/j.celrep.2015.12.082

Matharu, N., & Ahituv, N. (2015). Minor Loops in Major Folds: Enhancer–Promoter Looping, Chromatin Restructuring, and Their Association with Transcriptional Regulation and Disease. *PLoS Genetics*, *11*(12). https://doi.org/10.1371/journal.pgen.1005640

Matsushita, H., Nakajima, H., Nakamura, Y., Tsukamoto, H., Tanaka, Y., Jin, G., … Miyachi, H. (2008). C/EBPα and C/EBPε induce the monocytic differentiation of myelomonocytic cells with the MLL-chimeric fusion gene. *Oncogene*, *27*(53), 6749–6760. https://doi.org/10.1038/onc.2008.285

Matsuzaki, Y., Kinjo, K., Mulligan, R. C., & Okano, H. (2004). Unexpectedly Efficient Homing Capacity of Purified Murine Hematopoietic Stem Cells. *Immunity*, *20*(1), 87–93. https://doi.org/10.1016/S1074-7613(03)00354-6

Mazumdar, C., Shen, Y., Xavy, S., Zhao, F., Reinisch, A., Li, R., … Majeti, R. (2015). Leukemia-Associated Cohesin Mutants Dominantly Enforce Stem Cell Programs and Impair Human Hematopoietic Progenitor Differentiation. *Cell Stem Cell*, *17*(6), 675–688. https://doi.org/10.1016/j.stem.2015.09.017

Milne, T. A., Martin, M. E., Brock, H. W., Slany, R. K., & Hess, J. L. (2005). Leukemogenic MLL fusion proteins bind across a broad region of the Hox a9 locus, promoting transcription and multiple histone modifications. *Cancer Research*, *65*(24), 11367–11374. https://doi.org/10.1158/0008-5472.CAN-05-1041

Mirny, L. A., Goloborodko, A., Imakaev, M., Abdennur, N., Lu, C., & Fudenberg, G. (2016). Formation of Chromosomal Domains by Loop Extrusion. *Cell Reports*, *15*(9), 2038–2049. https://doi.org/10.1016/j.celrep.2016.04.085

Moore, J. M., Rabaia, N. A., Smith, L. E., Fagerlie, S., Gurley, K., Loukinov, D., … Filippova, G. N. (2012). Loss of maternal CTCF is associated with peri-implantation lethality of CtCf null embryos. *PLoS ONE*, *7*(4). https://doi.org/10.1371/journal.pone.0034915

Moretti, P., Simmons, P., Thomas, P., Haylock, D., Rathjen, P., Vadas, M., & D'Andrea, R. (1994). Identification of homeobox genes expressed in human haemopoietic progenitor cells. *Gene*, *144*(2), 213–219. https://doi.org/10.1016/0378-1119(94)90380-8

Morrison, S. J., Wandycz, A. M., Hemmati, H. D., Wright, D. E., & Weissman, I. L. (1997). Identification of a lineage of multipotent hematopoietic progenitors. *Development*, *124*(10), 1929–1939. Retrieved from http://www.ncbi.nlm.nih.gov/pubmed/9169840

Nakamura, T., Largaespada, D. A., Lee, M. P., Johnson, L. A., Ohyashiki, K., Toyama, K., … Shaughnessy, J. D. (1996). Fusion of the nucleoporin gene NUP98 to HOXA9 by the chromosome translocation t(7;11)(p15;p15) in human myeloid leukaemia. *Nature Genetics*, *12*(2), 154–158. https://doi.org/10.1038/ng0296-154

Narendra, V., Bulajié, M., Dekker, J., Mazzoni, E. O., & Reinberg, D. (2016). CTCF-mediated topological boundaries during development foster appropriate gene regulation. *Genes and Development*, *30*(24), 2657–2662. https://doi.org/10.1101/gad.288324.116

Narendra, V., Rocha, P. P., An, D., Raviram, R., Skok, J. A., Mazzoni, E. O., & Reinberg, D. (2015). CTCF establishes discrete functional chromatin domains at the Hox clusters during differentiation. *Science*, *347*(6225), 1017–1021. https://doi.org/10.1126/science.1262088

Ng, Y. Y., Baert, M. R. M., de Haas, E. F. E., Pike-Overzet, K., & Staal, F. J. T. (2009). Isolation of Human and Mouse Hematopoietic Stem Cells. In C. Baum (Ed.), *Genetic Modification of Hematopoietic Stem Cells: Methods and Protocols* (pp. 13–21). Totowa, NJ: Humana Press. https://doi.org/10.1007/978-1-59745-409-4_2

Nora, E. P., Goloborodko, A., Valton, A. L., Gibcus, J. H., Uebersohn, A., Abdennur, N., … Bruneau, B. G. (2017). Targeted Degradation of CTCF Decouples Local Insulation of Chromosome Domains from Genomic Compartmentalization. *Cell*, *169*(5), 930-944.e22. https://doi.org/10.1016/j.cell.2017.05.004

Nora, E. P., Lajoie, B. R., Schulz, E. G., Giorgetti, L., Okamoto, I., Servant, N., … Heard, E. (2012). Spatial partitioning of the regulatory landscape of the X-inactivation centre. *Nature*, *485*(7398), 381–385. https://doi.org/10.1038/nature11049

Okada, Y., Feng, Q., Lin, Y., Jiang, Q., Li, Y., Coffield, V. M., … Zhang, Y. (2005). hDOT1L links histone methylation to leukemogenesis. *Cell*, *121*(2), 167–178. https://doi.org/10.1016/j.cell.2005.02.020

Osawa, M., Hanada, K. I., Hamada, H., & Nakauchi, H. (1996). Long-term lymphohematopoietic reconstitution by a single CD34- low/negative hematopoietic stem cell. *Science*, *273*(5272), 242–245.

https://doi.org/10.1126/science.273.5272.242
Ouboussad, L., Kreuz, S., & Lefevre, P. F. (2013). CTCF depletion alters chromatin structure and transcription of myeloid-specific factors. *Journal of Molecular Cell Biology*, *5*(5), 308–322. https://doi.org/10.1093/jmcb/mjt023
Papaemmanuil, E., Gerstung, M., Bullinger, L., Gaidzik, V. I., Paschka, P., Roberts, N. D., … Campbell, P. J. (2016). Genomic classification and prognosis in acute myeloid leukemia. *New England Journal of Medicine*, *374*(23), 2209–2221. https://doi.org/10.1056/NEJMoa1516192
Phillips-Cremins, J. E., Sauria, M. E. G., Sanyal, A., Gerasimova, T. I., Lajoie, B. R., Bell, J. S. K., … Corces, V. G. (2013). Architectural protein subclasses shape 3D organization of genomes during lineage commitment. *Cell*, *153*(6), 1281–1295. https://doi.org/10.1016/j.cell.2013.04.053
Pietras, E. M., Reynaud, D., Kang, Y. A., Carlin, D., Calero-Nieto, F. J., Leavitt, A. D., … Passegué, E. (2015). Functionally Distinct Subsets of Lineage-Biased Multipotent Progenitors Control Blood Production in Normal and Regenerative Conditions. *Cell Stem Cell*, *17*(1), 35–46. https://doi.org/10.1016/j.stem.2015.05.003
Pope, B. D., Ryba, T., Dileep, V., Yue, F., Wu, W., Denas, O., … Gilbert, D. M. (2014). Topologically associating domains are stable units of replication-timing regulation Eukaryotic chromosomes replicate in a temporal order known as the replication-timing program. *Nature*. https://doi.org/10.1038/nature13986
Rao, R. C., & Dou, Y. (2015). Hijacked in cancer: The KMT2 (MLL) family of methyltransferases. *Nature Reviews Cancer*, *15*(6), 334–346. https://doi.org/10.1038/nrc3929
Rao, S. S. P., Huntley, M. H., Durand, N. C., Stamenova, E. K., Bochkov, I. D., Robinson, J. T., … Aiden, E. L. (2014). A 3D map of the human genome at kilobase resolution reveals principles of chromatin looping. *Cell*, *159*(7), 1665–1680. https://doi.org/10.1016/j.cell.2014.11.021
Rapin, N., Bagger, F. O., Jendholm, J., Mora-Jensen, H., Krogh, A., Kohlmann, A., … Porse, B. T. (2014). Comparing cancer vs normal gene expression profiles identifies new disease entities and common transcriptional programs in AML patients. *Blood*, *123*(6), 894–904. https://doi.org/10.1182/blood-2013-02-485771
Rice, K. L., & Licht, J. D. (2007). HOX deregulation in acute myeloid leukemia. *Journal of Clinical Investigation*, *117*(4), 865–868. https://doi.org/10.1172/JCI31861
Sive, J. I., Basilico, S., Hannah, R., Kinston, S. J., Calero-Nieto, F. J., & Gottgens, B. (2016). Genome-scale definition of the transcriptional programme associated with compromised PU.1 activity in acute myeloid leukaemia. *Leukemia*, *30*(1), 14–23. https://doi.org/10.1038/leu.2015.172
Sun, J., Ramos, A., Chapman, B., Johnnidis, J. B., Le, L., Ho, Y., … Harbor, C. S. (2014). Clonal dynamics of native haematopoiesis. *Nature*, *514*(7522), 322–327. https://doi.org/10.1038/nature13824.Clonal
Sun, Y., Zhou, B., Mao, F., Armstrong, S. A., Dou, Y., Hess, J. L., … Khoa, P. (2018). HOXA9 Reprograms the Enhancer Landscape to Promote Leukemogenesis. *Cancer Cell*, *34*(4), 643–658. https://doi.org/10.1016/j.ccell.2018.08.018
Svendsen, J. B., Baslund, B., Cramer, E. P., Rapin, N., Borregaard, N., & Cowland, J. B. (2016). MicroRNA-941 expression in polymorphonuclear granulocytes is not related to granulomatosis with polyangiitis. *PLoS ONE*, *11*(10), 1–12. https://doi.org/10.1371/journal.pone.0164985
Tang, Q., Iyer, S., Lobbardi, R., Moore, J. C., Chen, H., Lareau, C., … Langenau, D. M. (2017). Dissecting hematopoietic and renal cell heterogeneity in adult zebrafish at single-cell resolution using RNA sequencing. *Journal of Experimental Medicine*, *214*(10), 2875–2887. https://doi.org/10.1084/jem.20170976
Thol, F., Bollin, R., Gehlhaar, M., Walter, C., Dugas, M., Suchanek, K., … Heuser, M. (2014). Mutations in the cohesin complex in acute myeloid leukemia: clinical and prognostic implications. *Blood*, *123*(6), 914–921. https://doi.org/10.1182/blood-2013-07-518746.The
Thorsteinsdottir, U., Mamo, A., Kroon, E., Jerome, L., Bijl, J., Lawrence, H. J., … Sauvageau, G. (2002). Overexpression of the myeloid leukemia-associated Hoxa9 gene in bone marrow cells induces stem cell expansion. *Blood*, *99*(1), 121–129. https://doi.org/10.1182/blood.V99.1.121
van den Boom, V., Maat, H., Geugien, M., Rodríguez López, A., Sotoca, A. M., Jaques, J., … Schuringa, J. J. (2016). Non-canonical PRC1.1 Targets Active Genes Independent of H3K27me3 and Is Essential for Leukemogenesis. *Cell Reports*, *14*(2), 332–346. https://doi.org/10.1016/j.celrep.2015.12.034
Weissman, I. L. (2000). Stem cells: Units of development, units of regeneration, and units in evolution. *Cell*, *100*(1), 157–168. https://doi.org/10.1016/S0092-8674(00)81692-X
Wendt, K. S., Yoshida, K., Itoh, T., Bando, M., Koch, B., Schirghuber, E., … Peters, J. M. (2008). Cohesin mediates transcriptional insulation by CCCTC-binding factor. *Nature*. https://doi.org/10.1038/nature06634

Wierenga, A. T. J., Vellenga, E., & Schuringa, J. J. (2010). Down-regulation of GATA1 uncouples STAT5-induced erythroid differentiation from stem/progenitor cell proliferation. *Blood*, *115*(22), 4367–4376.

Xu, M., Zhao, G.-N., Lv, X., Liu, G., Wang, L. Y., Hao, D.-L., … Liang, C.-C. (2014). CTCF Controls HOXA Cluster Silencing and Mediates PRC2-Repressive Higher-Order Chromatin Structure in NT2/D1 Cells. *Molecular and Cellular Biology*, *34*(20), 3867–3879. https://doi.org/10.1128/mcb.00567-14

Yamamoto, R., Morita, Y., Ooehara, J., Hamanaka, S., Onodera, M., Rudolph, K. L., … Nakauchi, H. (2013). Clonal analysis unveils self-renewing lineage-restricted progenitors generated directly from hematopoietic stem cells. *Cell*, *154*(5), 1112–1126. https://doi.org/10.1016/j.cell.2013.08.007

Yi, G., Wierenga, A. T. J., Petraglia, F., Narang, P., Janssen-Megens, E. M., Mandoli, A., … Martens, J. H. A. (2019). Chromatin-Based Classification of Genetically Heterogeneous AMLs into Two Distinct Subtypes with Diverse Stemness Phenotypes. *Cell Reports*, *26*(4), 1059-1069.e6. https://doi.org/10.1016/j.celrep.2018.12.098

Zhang, Y., Gao, S., Xia, J., & Liu, F. (2018). Hematopoietic Hierarchy - An Updated Roadmap. *Trends in Cell Biology*, *0*(0), 1–11. https://doi.org/10.1016/j.tcb.2018.06.001

Zhu, N., Chen, M., Eng, R., DeJong, J., Sinha, A. U., Rahnamay, N. F., … Armstrong, S. A. (2016). MLL-AF9-and HOXA9-mediated acute myeloid leukemia stem cell self-renewal requires JMJD1C. *Journal of Clinical Investigation*, *126*(3), 997–1011. https://doi.org/10.1172/JCI82978

# Supplemental information

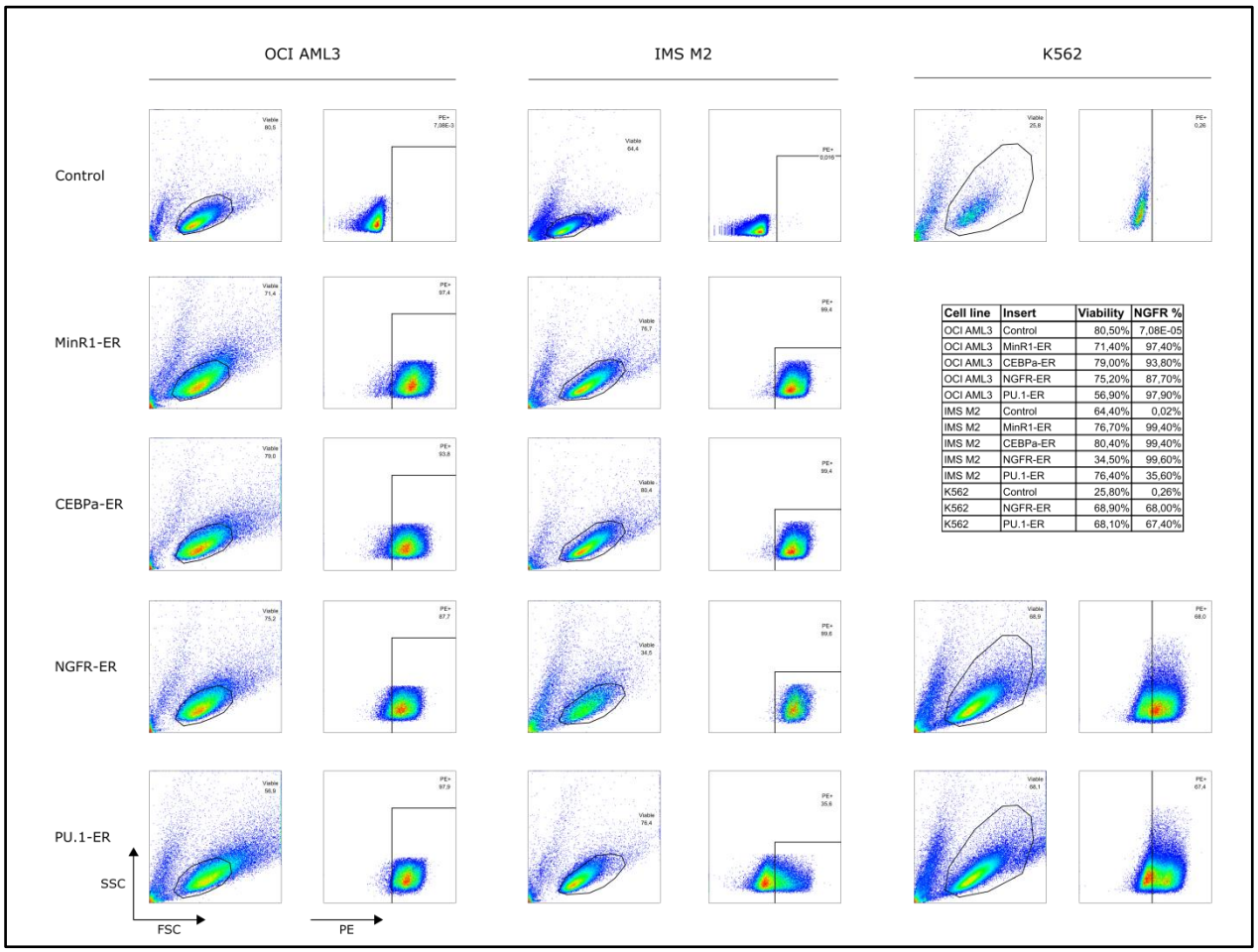


| Cell line | Insert | Viability | NGFR % |
|---|---|---|---|
| OCI AML3 | Control | 80,50% | 7,08E-05 |
| OCI AML3 | MinR1-ER | 71,40% | 97,40% |
| OCI AML3 | CEBPa-ER | 79,00% | 93,80% |
| OCI AML3 | NGFR-ER | 75,20% | 87,70% |
| OCI AML3 | PU.1-ER | 56,90% | 97,90% |
| IMS M2 | Control | 64,40% | 0,02% |
| IMS M2 | MinR1-ER | 76,70% | 99,40% |
| IMS M2 | CEBPa-ER | 80,40% | 99,40% |
| IMS M2 | NGFR-ER | 34,50% | 99,60% |
| IMS M2 | PU.1-ER | 76,40% | 35,60% |
| K562 | Control | 25,80% | 0,26% |
| K562 | NGFR-ER | 68,90% | 68,00% |
| K562 | PU.1-ER | 68,10% | 67,40% |

**Supplemental Figure 1.** Flow data of OCI AML3, IMS M2, and K562 after transduction with MinR1-ER, CEBPa-ER, NGFR-ER, and PU.1-ER. Cells were stained for 30 minutes with the CD271-PE antibody for the NGF receptor. Flow analysis was performed 3 months after transduction, and the NGFR positive gate was determined by comparison to untransduced cell lines.

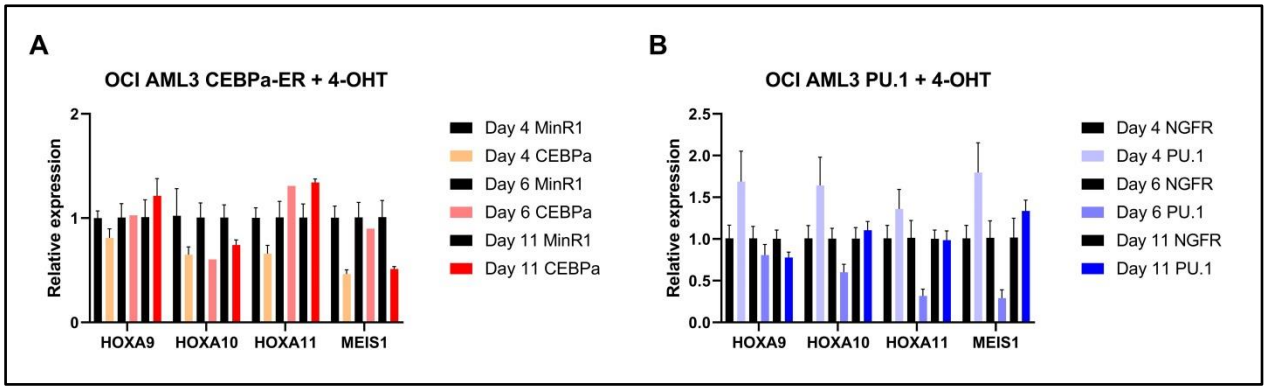


**Supplemental Figure 2. (A)** qPCR results of HOX genes in OCI AML3 CEBPa-ER. mRNA samples were taken after 4, 6, and 11 days with 4-OHT. **(B)** Same as A, but now in OCI AML3 PU.1-ER. mRNA samples were taken after 4, 6, and 11 days with 4-OHT.

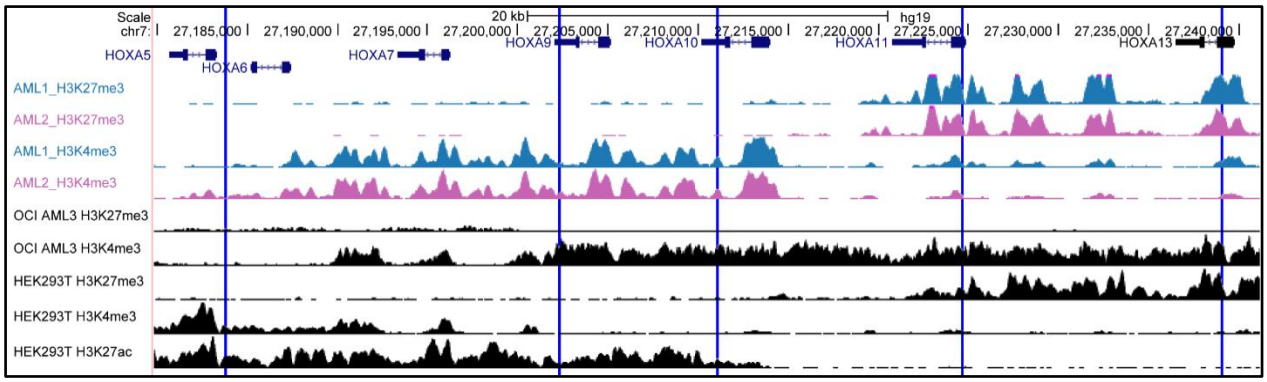


**Supplemental Figure 3.** ChIP locations for *HOXA5*, *HOXA9*, *HOXA10*, *HOXA11* and *HOXA13* across the *HOXA* locus. Shown are ChIP-seq results from 2 AML NPM1$^{cyt}$ patients (van den Boom et al., 2016), and the OCI AML3 (Brunetti et al., 2018) and HEK 293T (ENCODE) cell lines.

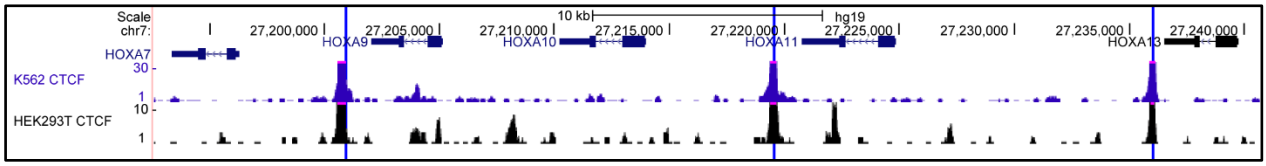


**Supplemental Figure 4.** ChIP locations for the CTCF binding sites between *HOXA7* and *HOXA9*, *HOXA10* and *HOXA11*, and nearby *HOXA13*. Shown are ChIP-seq results from K562 (ENCODE) and HEK 293T (ENCODE) cell lines.

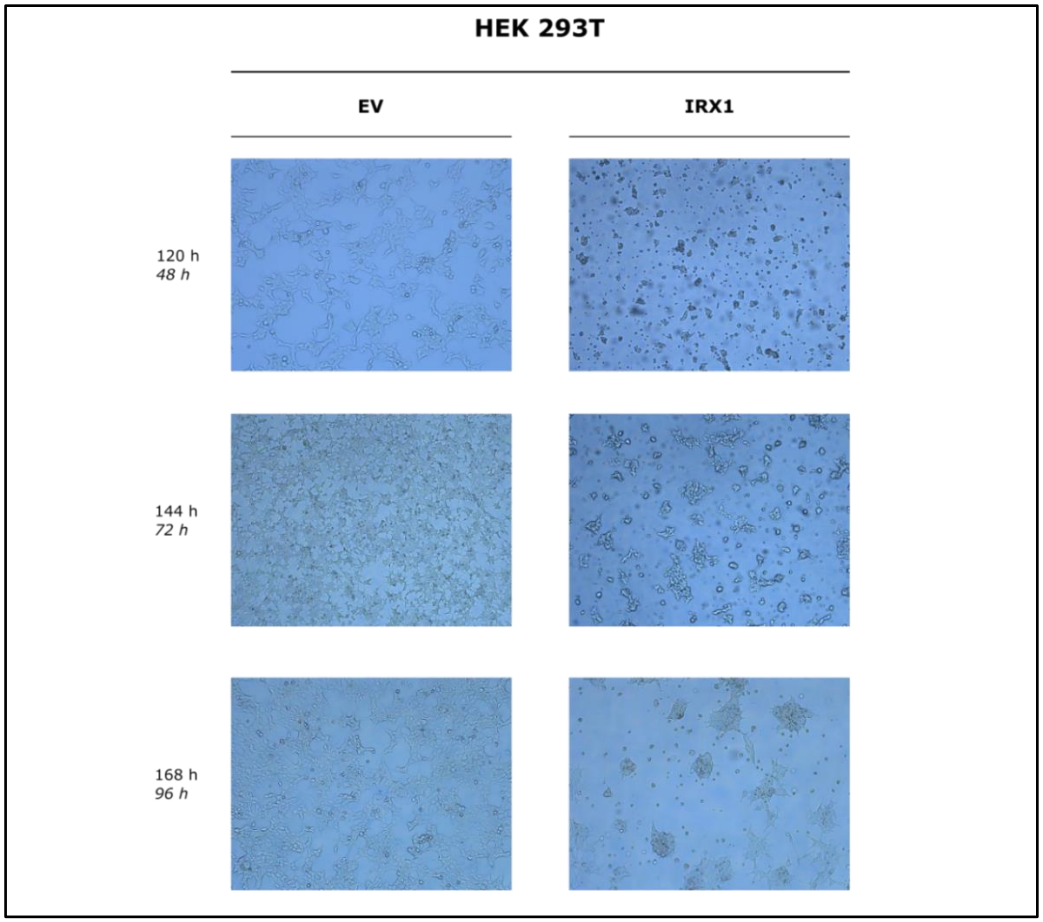


**Supplemental Figure 5.** HEK 293T cells 120, 144, and 168 hours post-transduction with IRX1 or EV. First pictures are 48 h after second passage, then 72 h, and 96 h.

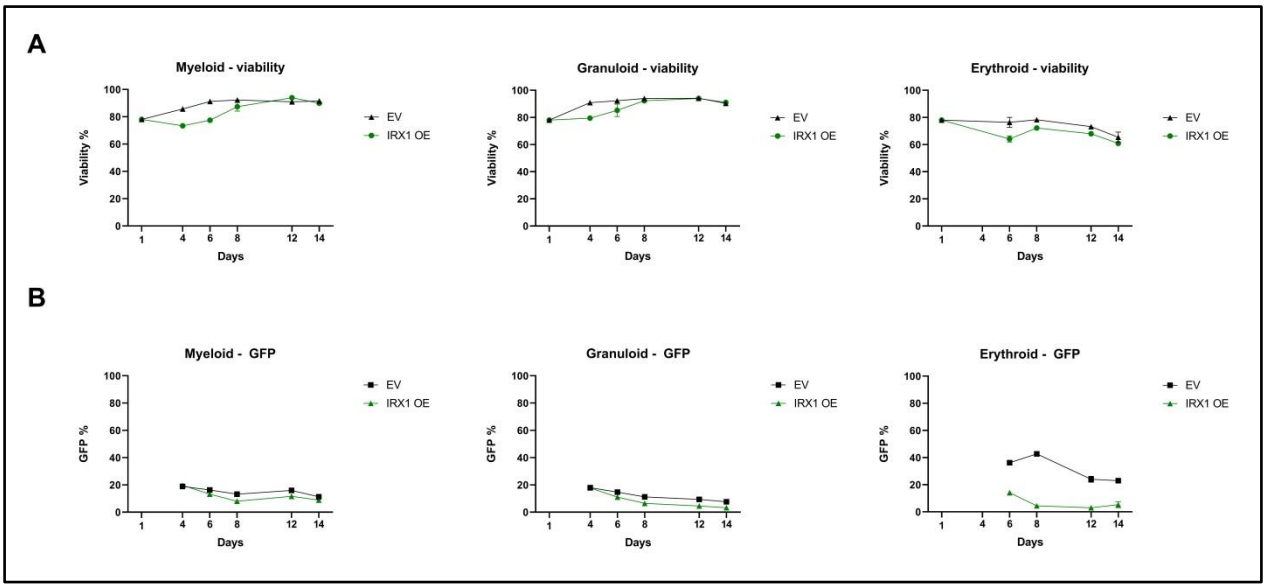


**Supplemental Figure 6.** CD34⁺ differentiation towards the myeloid, granulocytic, and erythroid lineage using cytokines. (A) Cell viability measured on LSR-II on day 4, 6, 12, and 14 for myeloid, granulocytic, and erythroid lineage. (B) Cell GFP % measured on LSR-II on day 4, 6, 12, and 14 for myeloid, granulocytic, and erythroid lineage.

### Supplemental table 1. List of primers

| Primer | Forward | Reverse |
|---|---|---|
| **ChIP primers** | | |
| **HOXA5** | CGACCCCAACCTCGACACAAAAATAAGAG | CAACAACTTTATTTCCCCCGTTTTGCAGC |
| **HOXA9** | TGGAGGAAATGAATGCTGATTGTAACGGAG | AGTAGCCCAATGGCGGTTTCATAGTG |
| **HOXA10** | ACAGCACTCCAGGCAGACAT | ATTGTTGGCGCTGAGGTGT |
| **HOXA11** | AGTATGTCATTGGGCGCGAA | ACGTCTCGGGTCCAGATTTC |
| **HOXA13** | CTGGTGGTAGAAGGCGAACTC | ACAAGTACATGGATACCGCCG |
| **EVX1** | GACTCCTTCCTCACCTTCGC | CCCTTATCTAGTGAGGGGCA |
| **CBS7/9** | GCAGAGGAGGCAATGCCAATAAAAGAG | TGTTCTGTCTGCCGCCGATAAAGC |
| **CBS10/11** | ATTGATCGGAAGTGCGCCATCTCG | ATCCTCTCCTCTCTCCTTCTCTCTCTGC |
| **CBS13** | GCGCCCTTGATCTACTAATCCAGCTAAG | TGACCTTGACTTTTGACAGCTCATGAATTG |
| **Expression primers** | | |
| **HOXA5** | AGATCTACCCCTGGATGCGC | CCTTCTCCAGCTCCAGGGTC |
| **HOXA7** | ATCACTCTACCTCGTAAAACCGAC | ACATAATACGAAGAACTCATAATTTTG |
| **HOXA9** | ACACTATGAAACCGCCATTGG | GGAAACCCCAGATTCATCAAGG |
| **HOXA10** | ATGATATGGCTTTTTCCCCCAG | TTCTTTGTGTTTGCTTGGTGCTG |
| **HOXA11** | GTCTTCCGGCCACACTGAG | ACGCTGAAGAAGAACTCCCG |
| **MEIS1** | GAACGAGTAGATGCCGTGTC | TCTGCCACCGGTATATTAGC |
| **RPL27** | TCCGGACGCAAAGCTGTCATCG | TCTTGCCCATGGCAGCTGTCAC |
| **CFS3R** | AGGCTACCCTCCAGCCATAC | ACGCAGTCCAGGATGGAGTC |
| **CT2** | CTTTGCACGCCAGGAAGGTC | CGCCGTAGTGTATGTGCTCG |
| **CALCR1** | CACTATGCCTGATGTGACGC | CATCAATGGTGTGCTGGAAC |

| | | |
|---|---|---|
| **PU.1** | GCGACCATTACTGGGACTTC | ATGGGTACTGGAGGCACATC |
| **SIRPA** | GTTTAAGTCTGGAGCAGGCACT | GCAGATGACTTGAGAGTGAACG |
| **RAD21** | TCATGGTCTTCAGCGTGCTC | TCCAGGTGTTGCGATGATGT |
| **CTCF** | GGAGCCTGCCGTAGAAATTG | TAGCTGTTGGCTGGTTCTGT |
| **SMC1A** | GGCGCCAACAAGGAAATGAC | CATGGTGCCTTTTGACAGTGG |
| **SMC3** | AGAAACAGAGGGCAAACGGG | AGCTCATCAAGTTTGGCACG |
| **STAG2** | TCGACATACAAGCACCCTGG | TCCTGAAGCTCTTTCCGCTT |

**Supplemental table 2. List of used antibodies**

| Antibodies | Source | Identifier |
|---|---|---|
| **Flow cytometry** | | |
| **CD34-APC** | BD Pharmingen™ | 555824 |
| **CD34-PeCy7** | BD Biosciences | 348811 |
| **CD34-BV421** | BD Horizon™ | 562577 |
| **CD38-FITC** | BD Pharmingen™ | 555459 |
| **CD38-PE** | BD Biosciences | 345806 |
| **CD11b-PeCy7** | Biolegend | 301322 |
| **CD11b-APC** | Biolegend | 301310 |
| **CD11b-PeCy5** | Biolegend | 301308 |
| **CD13-PE** | BD Pharmingen™ | 555394 |
| **CD14-PE** | Biolegend | 325606 |
| **CD15-APC** | BD Pharmingen™ | 551376 |
| **CD114-PE** | BD Pharmingen™ | 554538 |
| **CD71-PE** | BD Pharmingen™ | 555537 |
| **CD235a-APC** | Invitrogen | 17-9987-42 |
| **Western Blot** | | |
| **α-CEBPα** | Santa Cruz Biotechnology | Clone 14AA, sc-61 |
| **α-PU.1** | Santa Cruz Biotechnology | Clone T-21, sc-352 |
| **α-IRX1** | Abcam | ab98343 |
| **α-H3** | Abcam | ab1791 |
| **ChIP** | | |
| **α-H3K4me3** | Diagenode | C15410003-50 |
| **α-H3K27me3** | Diagenode | C15410195 |
| **α-H3K27ac** | Diagenode | C15410196 |
| **α-CTCF** | Abcam | ab70303 |
| **α-RAD21** | Abcam | ab992 |
| **IgG** | Sigma-Aldrich | I8140 |

**Supplemental table 3. ChIP buffers**

| | |
|---|---|
| **SDS Buffer (lysis buffer)** | 5.0ml 5M NACl (100mM final)<br>12.5ml 1M Tris-Cl, pH 8.1 (50mM Final)<br>2.5ml 0.5 EDTA, pH 8.0 (5mM Final)<br>500µl 10% NaN3 (0.2% Final)<br>12.5ml 10% SDS (0.5% Final)<br>add dH2O to 250ml |
| **Triton Dilution Buffer** | 25ml of 1M Tris-Cl, pH 8.6 (100mM Final)<br>5.0ml 5M NaCl (100mM Final)<br>2.5ml 0.5M EDTA, pH 8.0 (5mM Final)<br>500µl 10% NaN3 (0.2% Final)<br>62.5ml of 20% Triton X-100 (5.0% Final)<br>Add dH2O to 250ml |
| **Mixed Micelle Wash Buffer** | 15ml 5M NaCl (150mM Final)<br>10ml 1M Tris-Cl pH 8.1 (20 mM Final)<br>5ml 0.5M EDTA, pH 8.0 (5mM Final)<br>40ml 65% w/v sucrose<br>1ml 10% NaN3 (0.02% Final)<br>25ml 20% Triton X-100 (1% Final)<br>10ml 10% SDS (0.2% Final)<br>Add dH2O to 500 ml |
| **LiCl/detergent wash** | 25ml 10% deoxycholic acid (sodium salt) (0.5% w/v Final) or 2.5 g in 500ml<br>1ml 0.5M EDTA (1mM Final)<br>125ml 1M LiCl (250 mM Final)<br>2.5ml 100% NP-40 (o.5% w/v Final)<br>5ml 1M Tris-Cl, pH 8.0 (10 mM Final)<br>1ml 10% NaN3 (0.2% Final)<br>Add dH2O to 500 ml |
| **Buffer 500** | 50 ml 5M NaCl (500 mM Final)<br>0.5 g deoxycholic acid (sodium salt) in 500 ml<br>1ml EDTA 0.5M (1mM Final)<br>25ml 1M HEPES, pH 7,5 (50mM Final)<br>5ml 100% Triton X-100 (1% w/v Final)<br>1 ml 10% NaN3 (0.2% Final)<br>Add dH2O to 500 ml |
| **TE Buffer** | 10mM Tris-HCl pH 8.0<br>1mM EDTA (0.5M) |